Egr1 deficiency induces browning of inguinal subcutaneous white adipose tissue in mice

Cécile Milet[1*$], Marianne Bléher[1$], Kassandra Allbright[2], Mickael Orgeur[1], Fanny Coulpier[3], Delphine Duprez[1#*], Emmanuelle Havis[1#*]

[1] Sorbonne Universités, UPMC Univ Paris 06, CNRS UMR7622, Inserm U1156, IBPS-Developmental Biology Laboratory, F-75005 Paris, France.

[2] University of Pittsburgh, Pittsburgh, Pennsylvania, United States.

[3] École normale supérieure, PSL Research University, CNRS, Inserm, Institut de Biologie de l'École normale supérieure (IBENS), Plateforme Génomique, 75005 Paris, France.

[$] Co-first authors

[#] Co-senior authors

* Corresponding authors:

Emmanuelle Havis, emmanuelle.havis@upmc.fr, +33 1 44 27 34 40

Delphine Duprez, delphine.duprez@upmc.fr, +33 1 44 27 27 53

Running title: Egr1 and fat browning

Key words: Egr1, Ucp1, transcription, matrix, browning, adipocyte, mouse

Abstract

Beige adipocyte differentiation within white adipose tissue, referred to as browning, is seen as a possible mechanism for increasing energy expenditure. The molecular regulation underlying the thermogenic browning process has not been entirely elucidated. Here, we identify the zinc finger transcription factor EGR1 as a negative regulator of the beige fat program. Loss of *Egr1* in mice promotes browning in the absence of external stimulation and activates *Ucp1* that encodes the key thermogenic mitochondrial uncoupling protein-1. Moreover, EGR1 is recruited to the proximal region of the *Ucp1* promoter in subcutaneous inguinal white adipose tissue. Transcriptomic analysis of subcutaneous inguinal white adipose tissue in the absence of *Egr1* identifies the molecular signature of white adipocyte browning downstream of *Egr1* deletion and highlights a concomitant increase of beige differentiation marker and decrease in extracellular matrix gene expression. Conversely, *Egr1* overexpression in mesenchymal stem cells decreases beige adipocyte differentiation, while increasing extracellular matrix production. These results uncover the role of *Egr1* in blocking energy expenditure via direct *Ucp1* transcription regulation and highlight *Egr1* as a therapeutic target for counteracting obesity.

Introduction

White fat browning is a mechanism that produces heat and limits weight gain. The understanding of the molecular regulation underlying white fat browning has sparked interest to counteract obesity.

The adipose tissue of humans and other mammals contains white adipose tissue (WAT) and brown adipose tissue (BAT). WAT and BAT are developmentally and functionally distinct and contain white and brown adipocytes, respectively (Berry et al., 2013; Bartelt and Heeren 2014; Harms and Seale, 2013). More recently, a third type of adipocytes has been described within WAT, beige adipocytes. Morphological and molecular analyses showed that brown and beige adipocytes are remarkably similar and express the same thermogenic markers (Kajimura et al., 2015). However beige adipocytes, in contrast to brown adipocytes, express thermogenic markers only after external stimulations, such as cold exposure, starvation, exercise or hormone treatment (Rosenwald et al., 2013). In the adult, beige adipocytes are produced by the trans-differentiation of mature white adipocytes (Kajimura et al., 2015) or by *de novo* differentiation of progenitors (Wang et al., 2013) in response to external stimulations. This process is referred to as "browning" or "beigeing" (Bartelt and Heeren, 2014, Garcia et al., 2016).

Because the increase of WAT is observed in many metabolic diseases, WAT browning represents a promising therapeutic approach. Consequently, it is crucial to decipher the molecular aspects underlying the beige differentiation program. Adipogenesis is triggered by a common adipogenic network, starting with the expression of *Cebpb* (CCAAT/enhancer binding protein ß), which activates the expression of *Pparg (*Peroxisome proliferator-activated receptor γ) and *Cebpa* (CCAAT/enhancer binding protein α), which in turn activates *Ppara* (Peroxisome proliferator-activated receptor α) expression (Peirce et al., 2014). Consistent with its thermogenic function, brown/beige differentiated adipocytes express high levels of UCP1, a mitochondrial protein that uncouples oxidative phosphorylation from ATP synthesis (Klaus et al., 1991; Shabalina et al., 2013). The Krebs cycle enzymes, such as OGDH (oxoglutarate dehydrogenase), SUCLA2 (succinate-Coenzyme A ligase) and COX8B (Cytochrome C Oxidase Subunit VIIIb) (Forner et al., 2009; Wu et al., 2012) are also involved in heat production in beige/brown adipose tissue. Consistent with their anti-fat function, brown/beige differentiated adipocytes express factors involved in lipolysis such as PLIN5 (Perilipin 5; Gallardo-Montejano et al., 2016) and CIDEA (Cell Death-Inducing DFFA-Like Effector A; Wu et al., 2012). Beige adipocyte differentiation relies on the expression of a set of transcriptional activators (Bartelt and

Heeren 2014; Harms and Seale 2013). PRDM16 (PR domain containing 16) is considered as a master regulator of the brown/beige program via direct interaction with transcription factors, such as C/EBPβ, PPARα, PPARγ, and PGC-1α (Peroxisome proliferator-activated receptor Gamma Coactivator 1-alpha) (Rajakumari et al., 2013; Seale et al., 2011; Puigserver et al., 1998). Of note, beige and white differentiation programs share transcriptional regulators, such as C/EBPβ, which has been shown to be sufficient for *Ucp1* transcription via direct binding to *Ucp1* proximal promoter in vitro (Yubero et al., 1994; reviewed in Villarroya et al., 2016). Moreover, *Cebpb* mutant mice display defective thermoregulation (Carmona et al., 2005). In addition to transcriptional regulators, growth factors such as FGF21 (Fibroblast Growth Factor-21) and BMP4 (Bone morphogenetic Protein-4), adipokines such as leptin and hormones such as T_3 (Triiodothyronin 3) have been identified as being able to induce the brown/beige fat phenotype (Bartelt and Heeren, 2014; Kim and Plutzky, 2016; Forest et al., 2016). The T_4 to T_3 converting enzyme Desiodase 2 (DIO2) is also involved in the browning process (De Jesus et al., 2001).

The zinc finger transcription factor EGR1 (Early Growth Response-1) is involved in multiple processes including cell proliferation, differentiation, migration, apoptosis, and inflammation (Beckmann and Wilce, 1997; Cao et al., 1993; Pagel and Deindl, 2011; Sakamoto et al., 1994; Tsai-Morris et al., 1988) in many cell types. *Egr1* is expressed in adult adipose tissues (Yu et al., 2011; Zhang et al., 2013), where its overexpression has been linked to obesity in both humans and mouse models (Yu et al., 2011; Zhang et al., 2013). Consistently, EGR1 inhibits lipolysis and promotes fat accumulation in cultured adipocytes by directly repressing the transcription of the adipose triglyceride lipase (ATGL) gene (Chakrabarti et al., 2013).

In this study, we analysed the consequences of *Egr1* inhibition for subcutaneous inguinal white adipose tissue (SC-WAT) formation during postnatal and adult periods, using a mouse model deficient for *Egr1*, with no external stimulation. We also assessed the consequences of *Egr1* overexpression for beige differentiation in mesenchymal stem cells.

Results and Discussion

Egr1$^{-/-}$ mice display inguinal subcutaneous white adipose tissue browning with no external stimulation

The subcutaneous inguinal white adipose tissue (SC-WAT) expands during the post-natal period (Cereijo et al., 2014) and is the largest white fat depot in mice (Shabalina et al., 2013; Waldén et al., 2012). *Egr1* expression in SC-WAT was detected in blood vessels (Figure 1D, arrow a) as previously described (Khachigian et al., 1996) and in white adipocytes (Figure 1D, arrows b,c). The weight of SC-WAT fat pads was similar in *Egr1*$^{+/+}$ and *Egr1*$^{-/-}$ 4-month-old mice, although the total body weight was slightly reduced in *Egr1*$^{-/-}$ mice compared to control mice (Figure 1A-C). SC-WAT from 1-month-old (post-natal) and 4-month-old (adult) *Egr1*$^{-/-}$ mice exhibited high number of beige adipocytes, labelled with UCP1, compared to *Egr1*$^{+/+}$ mice (Figure 1E,F). Consistently, the *Ucp1* mRNA expression levels were increased in *Egr1*-deficient SC-WAT compared to equivalent control SC-WAT (Figure 1H). The density of adipocytes increased in SC-WAT of *Egr1*$^{-/-}$ mice compared to *Egr1*$^{+/+}$ mice with a significant increase of the proportion of beige adipocytes and thus a reduction in the proportion of white adipocytes (Figure 1G). Cell counts are compatible with two mechanisms for WAT browning described in the literature (Kajimura et al., 2015, Wang et al., 2013), trans-differentiation of white adipocytes and proliferation of beige cells. The increase of *Ucp1* transcript levels, of UCP1 protein and in the density of UCP1+ cells in SC-WAT of *Egr1*$^{-/-}$ mice (Figure 1) is consistent with the UCP1 increase previously observed in *Egr1*$^{-/-}$mice under high fat diet feeding (Zhang et al., 2013). It has to be noted that there was no need of any high fat diet to observe *Ucp1*/UCP1 increase in SC-WAT fat pads of our *Egr1*$^{-/-}$ mice. We conclude that *Egr1* deficiency promotes spontaneous WAT browning without external stimulation. These results indicate that the presence of *Egr1* in white adipocytes represses WAT browning.

Molecular signature of inguinal subcutaneous white adipose tissue browning downstream of *Egr1*

In order to define the molecular signature underlying WAT browning downstream of Egr1, we performed RNA-sequencing of SC-WAT of 2-week-old *Egr1*$^{+/+}$ and *Egr1*$^{-/-}$ mice. 336 differentially expressed genes were significantly detected in *Egr1*-deficient SC-WAT compared to control SC-WAT. The 132 upregulated differentially expressed genes (Figure 2A, Figure 2-figure supplement 1) were subjected to functional annotation clustering according to their Gene Ontology (GO) classification, in the "*Biological Process*" category (Figure 2-figure supplement

2). Among the 132 upregulated genes, the GO terms "*NADH metabolic process*", "*Tricarboxylic acid cycle*", "*Brown fat cell differentiation*" and "*Fatty acid metabolic process*" exhibited the highest enrichment scores (Figure 2-figure supplement 2). Consistent with the beige phenotype (Figure 1), the key beige adipocyte markers, *Ppargc1a, Ucp1*, *Cox8b*, *Cidea* (Garcia et al., 2016) and other genes known to be involved in the beige differentiation program, *Dio2*, *Pank1*, *Plin5*, *Ogdh* and *Sucla2* (De Jesus et al., 2001; Christian, 2014; Rosell et al., 2014; Forner et al., 2009) were identified as upregulated genes (Figure 2A). The increased expression of these beige genes was confirmed by RT-qPCR at 2 weeks and 4 months (Figure 2B,C). In addition, the generic adipogenesis regulators also known to be involved in beige differentiation, *Cepbb* (Kajimura et al., 2009) and *Ppara* (Barberá et al., 2001) displayed an increased expression in *Egr1*-deficient SC-WAT (Figure 2A-C). Interestingly, there was no modification of expression of signalling molecules controlling beige differentiation such as FGF21, BMP4 or Leptin. This indicates that EGR1 negatively regulates the transcription of beige differentiation markers. To test whether this regulation was direct, we performed Chromatin immunoprecipitation (ChIP) experiments from the SC-WAT of 2-week-old mice on key beige markers. EGR1 was recruited to the *Ucp1* proximal promoter in SC-WAT (Figure 2D), showing a direct transcriptional regulation by EGR1. EGR1 was also recruited to the *Cebpb* promoter but not to that of *Ppapgc1* gene (Figure 2D), highlighting a direct and an indirect transcriptional regulation of these two genes by EGR1. These results show that EGR1 exerts its transcriptional repression of the beige program at two levels at least, through the direct recruitment of the main beige differentiation marker *Ucp1* and also through the direct recruitment to the *Cebpb* gene, which is known to regulate *Ucp1* transcription (Yubero et al., 1994).

The 204 downregulated differentially expressed genes (Figure 3A, Figure 3-figure supplement 1) in SC-WAT of *Egr1*$^{-/-}$ mice were enriched for the GO terms "*Collagen fibril organization*", "*Collagen catabolic process*" and "*Extracellular matrix organization*" (Figure 3-figure supplement 2). WAT produces extracellular matrix (ECM) whose composition and remodelling is crucial for adipocyte function (Mariman and Wang, 2010). Conversely, the expansion of adipose tissue during obesity leads to tissue remodelling and is associated with overexpression of *Col1a1*, *Col5a2*, *Fn1*, *Dcn* and the matrix metalloprotease *Mmp2* genes (Divoux and Clement, 2011; Berger et al., 2015; Bolton et al., 2008; Dubois et al., 2008; Henegar et al., 2008). In the transcriptome of *Egr1*-deficient SC-WAT, *Col1a1*, *Col1a2*, *Col5a2*, *Col14a1*, *Fn1*, *Post*, *Dcn* and *Mmp2* were downregulated (Figure 3A), which was confirmed by RT-qPCR in SC-WAT of 2 week- and 4 month-old mice (Figures 3B,C). We conclude that *Egr1*-deficiency represses ECM genes associated with obesity.

The concomitant upregulation of beige differentiation genes and downregulation of ECM genes is a signature of WAT browning downstream of *Egr1* deletion without any external stimulation.

Forced *Egr1* expression in mouse mesenchymal stem cells reduces beige marker expression and promotes extracellular matrix gene expression

The spontaneous WAT browning in *Egr1*$^{-/-}$ mice and the direct transcriptional regulation of *Ucp1* gene by EGR1 in SC-WAT suggested that EGR1 repressed beige adipocyte differentiation. EGR1 gain-of-function experiments were performed in mouse mesenchymal stem cells, C3H10T1/2 cells, cultured under beige adipocyte differentiation conditions. Consistent with the increase in the number of adipocytes in SC-WAT of *Egr1*$^{-/-}$ (Figure 1), we observed a decreased number of C3H10T1/2-Egr1 cells compared to C3H10T1/2 cells after 8 days of culture in the beige differentiation medium (Figure 4A,B). Under beige stimulation, C3H10T1/2 cells acquired a beige phenotype, visualized by the appearance of numerous small lipid droplets and UCP1 expression within their cytoplasm (Figure 4A). In contrast, C3H10T1/2-Egr1 cells did not express UCP1 under beige stimulation, showing that EGR1 repressed the expression of the key thermogenic beige marker (Figure 4A). Consistent with the absence of UCP1 protein (Figure 4A), *Ucp1* mRNA levels were never increased in the presence of EGR1 (Figure 4C). This fits with EGR1 recruitment to *Ucp1* promoter in SC-WAT (Figure 2D). However, small lipid droplets were still observed in C3H10T1/2-Egr1 cells, indicating that EGR1 repressed part of the beige phenotype through the repression of UCP1, but did not fully abolish the formation of lipid droplets (Figure 4A). The expression of *Cebpb* and *Ppara* genes was significantly reduced in C3H10T1/2-Egr1 cells compared to control cells as that of *Cidea*, *Ogdh, Pank1*, *Sucla2* and *Plin5* genes (Figure 4C, Figure 4-figure supplement 1E). This showed that beige differentiation and the heat-producing ability of C3H10T1/2 cells were impaired upon EGR1 overexpression. EGR1 overexpression also blocked white adipocyte differentiation in C3H10T1/2 cells (Figure 4-figure supplement 1A-D), as previously observed (Guerquin et al., 2013). The inhibition of both beige and white differentiation programs by EGR1 is to be related with the direct (*Cebpb)* and indirect transcriptional regulation of generic adipogenesis genes by EGR1 (Figure 2).

In order to assess whether EGR1 promotes the expression of ECM genes in mesenchymal stem cells in the context of adipocyte differentiation, we analysed the expression of *Col5a2*, *Fn1* and *Postn* in C3H10T1/2 and C3H10T1/2-*Egr1* cells during beige (Figure 4C, Figure 4-figure supplement 1E) and white (Figure 4-figure supplement 1D) adipocyte differentiation. The expression of *Col5a2*, *Fn1* and *Postn* genes was upregulated in *Egr1* overexpressing cells,

showing that EGR1 activated the expression of ECM genes during adipocyte differentiation. The positive regulation of ECM genes by EGR1 during adipocyte differentiation was consistent with similar regulation in the context of fibrosis, atherosclerosis and tendon repair (Guerquin et al. 2013; Buechler et al. 2015). We conclude that forced EGR1 expression in mouse mesenchymal stem cells reduces beige marker expression, while promoting ECM gene expression.

In summary, the deletion of *Egr1* induces WAT browning through recruitment to the *Cebpb* and *Ucp1* promoters in mice without any cold stimulation or fasting (Figure 5). The upregulated expression profile of beige differentiation markers and downregulated profile of ECM genes in *Egr1*-deficient WAT define a molecular signature of beige adipocyte differentiation program and constitute a protective signature against white adipocyte lipid accumulation. This study identifies *Egr1* deficiency as a therapeutic approach to counteract obesity.

Materials and Methods

Mouse lines

The *Egr1* gene was inactivated by homologous recombination with insertion of the *LacZ* coding sequence within the *Egr1* 5' untranslated region in addition to a frameshift mutation upstream of the DNA-binding domain of *Egr1* (Topilko et al. 1998). The line was maintained on a C57BL/6J background (Janvier, France). All animals were kept under controlled photo-period (lights on 08:00–20:00 hours) and a diet of commercial rodent chow and tap water *ad libitum*. All procedures using mice were conducted in accordance with the guidelines of the French National Ethic Committee for animal experimentation N°05 and are registered under the number 01789.02.

In situ hybridization to adipose tissue sections

Inguinal subcutaneous fat pads were isolated from 1-month-old female mice, fixed in 4% paraformaldehyde overnight and processed for in situ hybridization to 6 mm wax tissue sections as previously described (Bonnin et al., 2015). The digoxigenin-labeled mouse *Egr1* probe was used as described in Topilko et al., 1998.

RNA isolation, sequencing and transcriptomic analysis

Fresh inguinal subcutaneous fat pads were removed from 2-week-old and 4-month-old euthanized *Egr1*$^{+/+}$ and *Egr1*$^{-/-}$ female mice and homogenized using a mechanical disruption device (Lysing Matrix A, Fast Prep MP1, 4 × 30 s, 6 m.s^{-1}). Total RNA was isolated using the RNeasy mini kit (Qiagen) with 15 min of DNase I (Qiagen) treatment according to the manufacturer's protocol. Preparation of cDNA libraries and sequencing was performed at the "Ecole Normale Supérieure" Genomic Platform (Paris, France), from subcutaneous inguinal fat pads of three 2-week-old *Egr1*$^{+/+}$ mice and three 2-week-old *Egr1*$^{-/-}$ mice. Ribosomal RNA depletion was performed with the Ribo-Zero kit (Epicentre), using 500 ng of total RNA. Libraries were prepared using the strand specific RNA-Seq library preparation ScriptSeq V2 kit (Epicentre). 51-bp paired-end reads were generated using a HiSeq 1500 device (Illumina). A mean of 56.9 ± 6.3 million reads passing the Illumina quality filter were obtained for each of the 6 samples. Reads were mapped against the *mus musculus* reference genome (UCSC Dec. 2011, GRCm38/mm10) using TopHat v2.1.0 (Kim et al., 2013), Bowtie (v2.2.5) (Langmead et al., 2012), and the Release M8 (GRCm38.p4) GTF annotations as a guide. Read counts were assigned to gene features using Feature Counts v1.4.6.p5 (Liao et al., 2014) and differential expression analysis was performed with DESeq2 v1.6.3 (Love et al., 2014). Full details of the Galaxy workflow used in this study can be retrieved via the following link: https://mississippi.snv.jussieu.fr/u/emmanuellehavis/w/copy-of-grasostendon-differential-expression-2. Gene Ontology analysis on differentially expressed genes (Padj<0.05) was performed with DAVID Bioinformatic Resources 6.8 (Huang et al., 2009). Sequencing data was uploaded to the Gene Expression Omnibus (GEO) database under the accession number GSE91058.

Chromatin Immunoprecipitation

ChIP assays were performed with previously reported protocol (Havis et al., 2006) on the inguinal subcutaneous adipose tissue isolated from sixty 2-week-old mice, homogenized using a mechanical disruption device (Lysing Matrix A, Fast Prep MP1, 3x30 sec). Eight micrograms of the rabbit polyclonal anti-Egr-1/Krox24 (C-19) antibody (Santa Cruz Biotechnology) or 8μg of the goat anti-mouse IgG2b (Southern biotechnology) were used to immunoprecipitate 30μg of sonicated chromatin. ChIP products were analyzed by quantitative PCR. 15μg of chromatin was isolated before chromatin immunoprecipitation, to be used as positive control for the PCR experiments (Input). ChIP products and Inputs were analyzed by quantitative PCR to amplify the promoter regions upstream the

Cebpb (-660bp; -530bp), *Ppargc1a* (-860bp; -730bp), *Ucp1* (-170bp; +20bp) *and Gapdh* (-2,9Kb; -2,7Kb; negative control) coding sequences. The primer list is displayed in Supplementary table 1.

Cell cultures

Mouse mesenchymal stem cells, C3H10T1/2 (Reznikoff et al. 1973) and the stable *Egr1* overexpressing counterparts, C3H10T1/2-Egr1 (Guerquin et al. 2013) cells, were plated on 6-well plates at a density of 33,000 cells/well and grown in Dulbecco's Modified Eagle's Medium (DMEM, Invitrogen) supplemented with 10% foetal bovine serum (FBS, Sigma), 1% penicillin-streptomycin (Sigma), 1% Glutamin (Sigma), 800 µg/ml G418 Geneticin (Sigma) and incubated at 37 °C in humidified atmosphere with 5% CO2.

Confluent cells were cultured in beige differentiation induction medium for 2 days and in beige maturation medium for 6 days according to published protocols (Lone et al., 2015). Day 0 corresponds to the addition of beige differentiation induction medium on confluent cells. Beige differentiation induction medium includes DMEM, 10% FBS, 1% penicillin-streptomycin, 10 μg/mL Insulin (Sigma), 0.25 μM Dexamethasone (Sigma), 0.5 mM 3-Isobutyl-1-methylxanthine (IBMX, Sigma), 50 nM 3.3',5-Triiodo-L-thyronine sodium salt (T_3, Sigma), 20 μM Curcumin (Sigma). The beige maturation medium comprises DMEM, 10% FBS, 1% penicillin-streptomycin, 10 μg/mL Insulin (Sigma), 50 nM 3,3',5-Triiodo-L-thyronine sodium salt (T_3, Sigma), 20 μM Curcumin (Sigma), 1 μM Rosiglitazone (Sigma). The maturation medium was changed every 2 days. Cells subjected to beige adipocyte differentiation medium were fixed for histological analysis or lysed for gene expression analysis at Day 0, Day 1, Day 6 and Day 8.

Confluent cells were cultured in white differentiation induction medium for 2 days and in white maturation medium for 8 days. Day 0 corresponds to the addition of white differentiation medium. White differentiation induction medium includes DMEM, 10% FBS, 1% penicillin-streptomycin, 10 μg/mL Insulin (Sigma), 0.25 μM Dexamethasone (Sigma), 0.5 mM 3-Isobutyl-1-methylxanthine (IBMX, Sigma), 30 nM 3.3',5-Triiodo-L-thyronine sodium salt (T_3, Sigma). The white maturation medium comprises DMEM, 10% FBS, 1% penicillin-streptomycin and 10 μg/mL Insulin (Sigma). The maturation medium was changed every 2 days. Cells subjected to white adipocyte differentiation medium were stopped at Day 0, Day 1, Day 4 and Day 10 for histological and gene expression analysis.

Cell number measurements were performed using the free software Image J (Rasband, W.S., Image J, U. S. National Institutes of Health, Bethesda, Maryland, USA, http://imagej.nih.gov/ij/, 1997-2012).

Oil Red O staining

C3H10T1/2 and C3H10T1/2-Egr1 cells were cultured in beige or white adipocyte differentiation medium for 8 and 10 days, respectively. Cells were fixed with 4% Paraformaldehyde (Sigma) for 15 min and washed twice with excess distilled H_2O (Millipore). 60% Isopropanol was added for 5 min and replaced with an Oil Red O (Sigma) staining mixture, consisting of Oil Red O solution (0.5% Oil Red O dye in Isopropanol) and water in a 6:4 ratio, for 15 min. Cells were rinsed three times in distilled H_2O, followed by a standard Hematoxylin & Eosin staining protocol.

Immunohistochemistry

Fresh inguinal subcutaneous fat pads were removed from 1 and 4 month-old euthanized *Egr1*$^{+/+}$ and *Egr1*$^{-/-}$ female mice, fixed in 4% formaldehyde overnight at 4°C and processed for immunohistochemistry on 10 μm wax tissue sections, as previously described (Wang et al., 2010). After wax removal, heat-induced epitope retrieval was performed by incubating sections 5 min at 95°C in Glycine-HCl buffer (0.05M Glycine, pH3.5). UCP1 protein was detected using rabbit polyclonal antibody (1:200, ab10983, Abcam), followed by secondary anti-rabbit HRP conjugate antibody (1:200, 170-6515, Biorad) and DiaminoBenzidine Tetra-Hydrochloride protocol (DAB) staining. Hematoxylin & Eosin (H&E) histological staining was performed using a standard protocol. Cell number measurements were performed using the free software Image J (Rasband, W.S., Image J, U. S. National Institutes of Health, Bethesda, Maryland, USA, http://imagej.nih.gov/ij/, 1997-2012).

C3H10T1/2 and C3H10T1/2-Egr1 cells were cultured in beige or white adipocyte differentiation medium for 8 and 10 days, respectively, on cover slips. Cells were fixed with 4% Paraformaldehyde (Sigma) for 15 min. UCP1 protein was detected using rabbit polyclonal antibody (1:200, ab10983, Abcam), followed by secondary anti-rabbit HRP conjugate antibody (1:200, 170-6515, Biorad) and DiaminoBenzidine Tetra-Hydrochloride protocol (DAB) staining. Hematoxylin & Eosin (H & E) histological staining was performed using a standard protocol. Cell number measurements were performed using the free software Image J (Rasband, W.S., Image J, U. S. National Institutes of Health, Bethesda, Maryland, USA, http://imagej.nih.gov/ij/, 1997-2012).

Reverse-Transcription and quantitative real time PCR

For RT-qPCR analyses, 500 ng RNAs were Reverse Transcribed using the High Capacity Retrotranscription kit (Applied Biosystems). Quantitative PCR was performed using SYBR Green PCR Master Mix (Applied Biosystems) using primers listed in Supplementary Table 1. The relative mRNA levels were calculated using the $2^{-\Delta\Delta Ct}$ method (Livak and Schmittgen, 2001). The Cts were obtained from Ct normalized to *Rplp0*, *Rn18S* or *Actb* levels in each sample. For mRNA level analysis in SC-WAT, 5 to 7 independent RNA samples of 2-week-old and 4-month-old *Egr1*$^{+/+}$ and *Egr1*$^{-/-}$ female mice were analysed in duplicate. For mRNA level analysis of C3H10T1/2 and C3H10T1/2-Egr1 cell cultures, 6 independent RNA samples were analysed in duplicate for each time point.

Statistical analyses

Data was analysed using the non-parametric Mann-Withney test or ANOVA test with Graphpad Prism V6. Results are shown as means ± standard deviations. The p-values are indicated either with the value or with * or #.

Acknowledgements

We thank Kacey Marra, Peter Rubin and Erin Kershaw from the University of Pittsburgh Medical Center, Pittsburgh, Pennsylvania, United States for comments on the manuscript and their expertise in adipose tissue biology. We thank Estelle Hirsinger from IBPS, Paris, France for comments on the manuscript. We thank Marie-Ange Bonnin from IBPS, Paris, France for technical support. We thank Sophie Lemoine and Stéphane Le Crom, from IBENS, Paris, France and Christophe Antoniewsky from ARTbio Bioinformatics Analysis Facility, Paris, France, for the bioinformatics analyses of the RNA-sequencing. We thank Sophie Gournet for illustrations.

Competing interests

The authors declare no competing financial interests.

Author contributions

CM, acquisition, analysis and interpretation of data. KOA, contributed to unpublished essential data, analysis and interpretation of histology data, drafting the article. MO, analysis and interpretation of bioinformatics data. FC, acquisition of RNA-sequencing data. DD, conception, design, analysis and interpretation of data, drafting the article, funding. EH, conception, design, analysis and interpretation of data, drafting the article.

Funding

This work was supported by the Fondation pour la Recherche Médicale (FRM) DEQ20140329500 and FDT20150532272, Institut national de la santé et de la recherche Médicale (Inserm), Centre National de la Recherche Scientifique (CNRS), Université Pierre et Marie Curie (UPMC) and the Agence Nationale de la Recherche (contracts ANR-10-BLAN-1219, ANR- 12-BSV1-0038). The École normale supérieure genomic platform was supported by the France Génomique national infrastructure, funded as part of the "Investissements d'Avenir" program managed by the Agence Nationale de la Recherche (contract ANR-10-INBS-09).

References

Barberá MJ, Schluter A, Pedraza N, Iglesias R, Villarroya F, Giralt M. 2001. Peroxisome proliferator-activated receptor α activates transcription of the brown fat uncoupling protein-1 gene. A link between regulation of the thermogenic and lipid oxidation pathways in the brown fat cell. *Journal of Biological Chemistry*, 276(2), pp.1486–1493.

Bartelt A, Heeren J. 2014. Adipose tissue browning and metabolic health. *Nature reviews*. Endocrinology, 10(1), pp.24–36.

Beckmann AM, Wilce PA. 1997. Egr transcription factors in the nervous system. *Neurochemistry International*, 31(4), pp.477–51.

Berger E, Héraud S, Mojallal A, Lequeux C, Weiss-Gayet M, Damour O, Géloën A. 2015. Pathways commonly dysregulated in mouse and human obese adipose tissue: FAT/CD3613 modulates differentiation and lipogenesis. *Adipocyte*, 4(3), pp.161–80.

Berry DC, Stenesen D, Zeve D, Graff JM. 2013. The developmental origins of adipose tissue. *Development*, 140(19), pp.3939-49 140.

Bolton K, Segal D, McMillan J, Jowett J, Heilbronn L, Abberton K, Zimmet P, Chisholm D,

Collier G, Walder K. 2005. Decorin is a secreted protein associated with obesity and type 2 diabetes. *International journal of obesity*, 32(7), pp.1113–1121.

Bonnin MA, Laclef C, Blaise R, Eloy-Trinquet S, Relaix F, Maire P, Duprez D. 2005. Six1 is not involved in limb tendon development, but is expressed in limb connective tissue under Shh regulation. *Mech Dev*, 122(4):573-85.

Buechler C, Krautbauer S, Eisinger K. 2015. Adipose tissue fibrosis. *World journal of diabetes*, 6(4), pp.548–53.

Cao X, Mahendran R, Guy GR, Tan YH. 1993. Detection and characterization of cellular EGR-1 binding to its recognition site. *Journal of Biological Chemistry*, 268(23), pp.16949–16957.

Cereijo R, Giralt M, Villarroya F. 2014. Thermogenic brown and beige/brite adipogenesis in humans. *Annals of medicine*, 47(2), pp.169–77.

Chakrabarti P, Kim JY, Singh M, Shin YK, Kim J, Kumbrink J, Wu Y, Lee MJ, Kirsch KH, Fried SK, Kandror KV. 2013. Insulin inhibits lipolysis in adipocytes via the evolutionarily conserved mTORC1-Egr1- ATGL-mediated pathway. *Molecular and cellular biology*, 33(18), pp.3659–66.

Christian M. 2014. Transcriptional fingerprinting of "browning" white fat identifies NRG4 as a novel adipokine. *Adipocyte*, 4(1), pp.50–54.

Divoux A, Clement K. 2011. Architecture and the extracellular matrix: The still unappreciated components of the adipose tissue. *Obesity Reviews*, 12(501), pp.494–503.

Dubois SG, Tchoukalova YD, Heilbronn LK, Albu JB, Kelley DE, Smith SR, Fang X, Ravussin E. 2008. Potential role of increased matrix metalloproteinase-2 (MMP2) transcription in impaired adipogenesis in type 2 diabetes mellitus. *Biochemical and Biophysical Research Communications*, 367(4), pp.725–728.

Forest C, Joffin N, Jaubert AM, Noirez P. 2016. What induces watts in WAT? *Adipocyte*, 5(2), pp.136–152.

Forner F, Kumar C, Luber CA, Fromme T, Klingenspor M, Mann M. 2009. Proteome Differences between Brown and White Fat Mitochondria Reveal Specialized Metabolic Functions. *Cell Metabolism*, 10(4), pp.324–335.

Gallardo-Montejano VI, Saxena G, Kusminski CM, Yang C, McAfee JL, Hahner L, Hoch K, Dubinsky W, Narkar VA, Bickel PE. 2016. Nuclear Perilipin 5 integrates lipid droplet lipolysis with PGC-1α/SIRT1-dependent transcriptional regulation of mitochondrial function. *Nature Communications*, (7)12723.

Garcia RA, Roemmich JN, Claycombe KJ. 2016. Evaluation of markers of beige adipocytes

in white adipose tissue of the mouse. *Nutrition and metabolism*, 13(1), p.24.

Guerquin MJ, Charvet B, Nourissat G, Havis E, Ronsin O, Bonnin MA, Ruggiu M, Olivera-Martinez I, Robert N, Lu Y, Kadler KE, Baumberger T, Doursounian L, Berenbaum F, Duprez D. 2013. Transcription factor EGR1 directs tendon differentiation and promotes tendon repair. *Journal of Clinical Investigation*, 123(8), pp.3564-76.

Havis E, Anselme I, Schneider-Maunoury S. 2006. Whole embryo chromatin immunoprecipitation protocol for the in vivo study of zebrafish development. *Biotechniques*, 40(1):34, 36, 38

Harms M, Seale P. 2013. Brown and beige fat: development, function and therapeutic potential. *Nature medicine*, 19(10), pp.1252–63.

Henegar C, Tordjman J, Achard V, Lacasa D, Cremer I, Guerre-Millo M, Poitou C, Basdevant A, Stich V, Viguerie N, Langin D, Bedossa P, Zucker JD, Clement K. 2008. Adipose tissue transcriptomic signature highlights the pathological relevance of extracellular matrix in human obesity. *Genome Biology*, 9(1), pp.R14.

Huang da W, Sherman BT, Lempicki RA. 2009. Bioinformatics enrichment tools: paths toward the comprehensive functional analysis of large gene lists. *Nucleic Acids Research*, 37(1), pp.1-13.

de Jesus LA, Carvalho SD, Ribeiro MO, Schneider M, Kim SW, Harney JW, Larsen PR, Bianco AC. 2001. The type 2 iodothyronine deiodinase is essential for adaptive thermogenesis in brown adipose tissue. *Journal of Clinical Investigation*, 108(9), pp.1379–1385.

Kajimura S, Seale P, Kubota K, Lunsford E, Frangioni JV, Gygi SP, Spiegelman BM. 2009. Initiation of myoblast to brown fat switch by a PRDM16-C/EBP- beta transcriptional complex. *Nature*, 460(7259), pp.1154-8.

Kajimura S, Spiegelman BM, Seale P. 2015. Brown and beige fat: Physiological roles beyond heat generation. *Cell Metabolism*, 22(4), pp.546–559.

Khachigian LM, Lindner V, Williams AJ, Collins T. 1996. Egr-1-induced endothelial gene expression: a common theme in vascular injury. *Science*. 271(5254):1427-31.

Kim D, Pertea G, Trapnell C, Pimentel H, Kelley R, Salzberg SL. 2013. TopHat2: accurate alignment of transcriptomes in the presence of insertions, deletions and gene fusions. *Genome Biology*, 14(4)pp.R36.

Kim SH, Plutzky J. 2016. Brown Fat and Browning for the Treatment of Obesity and Related Metabolic Disorders. *Diabetes and metabolism journal*, 40(1), pp.12–21.

Klaus S, Casteilla L, Bouillaud F, Ricquier D. 1991. The uncoupling protein UCP: a membraneous mitochondrial ion carrier exclusively expressed in brown adipose tissue. *International Journal of Biochemistry*, 23(9), pp.791-801.

Langmead B, Salzberg SL. 2012. Fast gapped-read alignment with Bowtie 2. *Nature Methods*, 9(4), pp.357-9.

Liao Y, Smyth GK, Shi W. 2014. featureCounts: an efficient general purpose program for assigning sequence reads to genomic features. *Bioinformatics*, 30(7), pp.923-30.

Livak KJ, Schmittgen TD. 2001. Analysis of relative gene expression data using real-time quantitative PCR and the 2(-DD C(T)) Method. *Methods*. 25(4), pp.402-8.

Lone J, Choi JH, Kim SW, Yun JW. 2015. Curcumin induces brown fat-like phenotype in 3T3-L1 and primary white adipocytes. *Journal of Nutritional Biochemistry*, (27), pp.193-202.

Love MI, Huber W, Anders S. 2014. Moderated estimation of fold change and dispersion for RNA-seq data with DESeq2. *Genome Biology*, 15(12), pp.550.

Mariman EC, Wang P. 2010. Adipocyte extracellular matrix composition, dynamics and role in obesity. *Cellular and molecular life sciences*, 67(8), pp.1277–1292.

Pagel JI, Deindl E. 2011. Early growth response 1, a transcription factor in the crossfire of signal transduction cascades. *Indian journal of biochemistry and biophysics*, 48(4), pp.226–35.

Peirce V, Carobbio S, Vidal-Puig A. 2014. The different shades of fat. *Nature*, 510(7503), pp.76–83.

Puigserver P, Wu Z, Park CW, Graves R, Wright M, Spiegelman BM. 1998. A Cold-Inducible Coactivator of Nuclear Receptors Linked to Adaptive Thermogenesis. *Cell*, 92(6), pp.829-39

Rajakumari S, Wu J, Ishibashi J, Lim HW, Giang AH, Won KJ, Reed RR, Seale P. 2013. EBF2 determines and maintains brown adipocyte identity. *Cell Metabolism*, 17(4), pp.562–574.

Reznikoff CA, Brankow DW, Heidelberger C. 1973. Establishment and characterization of a cloned line of C3H mouse embryo cells sensitive to postconfluence inhibition of division. *Cancer Research*, 33(12), pp.3231-8.

Rosell M, Kaforou M, Frontini A, Okolo A, Chan YW, Nikolopoulou E, Millership S, Fenech ME, MacIntyre D, Turner JO, Moore JD, Blackburn E, Gullick WJ, Cinti S, Montana G, Parker MG, Christian M. 2014. Brown and white adipose tissues: intrinsic differences in gene expression and response to cold exposure in mice. *American journal of physiology. Endocrinology and metabolism*, 306(8), pp.E945-64.

Rosenwald M, Perdikari A, Rülicke T, Wolfrum C. 2013. Bi-directional interconversion of brite and white adipocytes. *Nature Cell Biology*, 15(6), pp.659–667.

Sakamoto KM, Fraser JK, Lee HJ, Lehman E, Gasson JC. 1994. Granulocyte-macrophage colony-stimulating factor and interleukin-3 signaling pathways converge on the CREB-binding site in the human egr-1 promoter. *Molecular and cellular biology*, 14(9), pp.5975–85.

Seale P, Conroe HM, Estall J, Kajimura S, Frontini A, Ishibashi J, Cohen P, Cinti S, Spiegelman BM. 2011. Prdm16 determines the thermogenic program of subcutaneous white adipose tissue in mice. *Journal of Clinical Investigation*, 121(1), pp.53–56.

Seale P., 2015. Transcriptional regulatory circuits controlling brown fat development and activation. *Diabetes*, 64(7), pp.2369–2375.

Shabalina IG, Petrovic N, de Jong JM, Kalinovich AV, Cannon B, Nedergaard J. 2013. UCP1 in Brite/Beige adipose tissue mitochondria is functionally thermogenic. *Cell Reports*, 5(5), pp.1196–1203.

Topilko P, Schneider-Maunoury S, Levi G, Trembleau A, Gourdji D, Driancourt MA, Rao CV, Charnay P. 1998. Multiple pituitary and ovarian defects in Krox-24 (NGFI-A, Egr- 1)-targeted mice. *Molecular endocrinology*, 12(1), pp.107–122.

Tsai-Morris CH, Cao XM, Sukhatme VP. 1988. 5' flanking sequence and genomic structure of Egr-1, a murine mitogen inducible zinc finger encoding gene. *Nucleic acids research*, 16(18), pp.8835–46.

Waldén TB, Hansen IR, Timmons JA, Cannon B, Nedergaard J. 2012. Recruited vs. nonrecruited molecular signatures of brown , "brite" and white adipose tissues. American journal of physiology. *Endocrinology and metabolism* 302(1), pp.E19-31.

Wang QA, Tao C, Gupta RK, Scherer PE. 2013. Tracking adipogenesis during white adipose tissue development, expansion and regeneration. *Nature Medicine*, 19(10), pp.1338-44.

Wu J, Boström P, Sparks LM, Ye L, Choi JH, Giang AH, Khandekar M, Virtanen KA, Nuutila P, Schaart G, Huang K, Tu H, van Marken Lichtenbelt WD, Hoeks J, Enerbäck S, Schrauwen P, Spiegelman BM. 2012. Beige adipocytes are a distinct type of thermogenic fat cell in mouse and human. *Cell*, 150(2), pp.366–376.

Yu X, Shen N, Zhang ML, Pan FY, Wang C, Jia WP, Liu C, Gao Q, Gao X, Xue B, Li CJ. 2011. Egr-1 decreases adipocyte insulin sensitivity by tilting PI3K/Akt and MAPK signal balance in mice. *EMBO Journal*, 30(18), pp.3754-65.

Zhang J, Zhang Y, Sun T, Guo F, Huang S, Chandalia M, Abate N, Fan D, Xin HB, Chen YE, Fu M. 2013. Dietary obesity-induced Egr-1 in adipocytes facilitates energy storage via

suppression of FOXC2. *Scientific reports*, (3) p.1476.

Figure legends

Figure 1. *Egr1* loss-of-function leads to inguinal subcutaneous white adipose tissue browning in postnatal and 4 month-old mice. (**A**) Pictures of fat pads (SC-WAT) from 4-month-old $Egr1^{+/+}$ and $Egr1^{-/-}$ mice. Scale bars: 5mm. (**B**) Weight in grams of SC-WAT of 4-month-old $Egr1^{+/+}$ and $Egr1^{-/-}$ mice. The graph shows mean ± standard deviations of 6 $Egr1^{+/+}$ fat pads and 8 $Egr1^{-/-}$ fat pads. (**C**) Weight in grams of 4-month-old wild-type and mutant mice. The graph shows means ± standard deviations of 4 $Egr1^{+/+}$ and 4 $Egr1^{-/-}$ mice. The p-value was obtained using the Mann-Whitney test. Asterisk indicates the p-value *P<0.05 . (**D**) SC-WAT of 1-month-old mouse was longitudinally sectioned. 6µm sections were hybridized with the DIG-labeled antisense probe for *Egr1* (blue). Arrow "a" points *Egr1* expression in blood vessels. Arrows "b" and "c" indicate *Egr1* expression in white adipocytes. Scale bars: 50µm. (**E,F**) Sections of SC-WAT of 1-month-old (**E**) and 4-month-old (**F**) $Egr1^{+/+}$ and $Egr1^{-/-}$ mice were immuno-stained with UCP1 antibody and counterstained with hematoxilin. Scale bars: lower magnification 100μm; intermediate magnification 50μm, higher magnification 25μm. (**G**) White and beige adipocyte number was counted in arbitrary unit areas of transverse sections of the SC-WAT of 1 month-old (N=7) and 4 month-old (N=8) $Egr1^{+/+}$ and $Egr1^{-/-}$ mice. Graphs show means of 7 or 8 sections for each sample ± standard deviations. Asterisks indicate the p-values obtained using the Mann-Whitney test, comparing beige or white adipocyte number between mutant and control mice *** P<0.001, **P<0.01. Number signs indicate the p-values obtained using Anova test comparing cell number between mutant and control mice ### P<0.001. (**H**) RT-qPCR analysis of expression levels for beige adipocyte differentiation marker *Ucp1* in SC-WAT of 2-week-old and 4-month-old $Egr1^{-/-}$ mice compared to $Egr1^{+/+}$ mice. The mRNA levels of control ($Egr1^{+/+}$) SC-WAT were normalized to 1. Graphs show means ± standard deviations of 7 samples from 2-week-old $Egr1^{+/+}$ mice, 5 samples from 2-week-old $Egr1^{-/-}$ mice and 5 samples from 4-month-old wild-type and mutant mice. The p-values were obtained using the Mann-Withney test. Asterisks indicate the p-values * p<0.05, ** p<0.01.

Figure 2. Transcriptomic analysis of subcutaneous inguinal adipose tissue of postnatal $Egr1^{-/-}$ versus $Egr1^{+/+}$ mice shows upregulation of beige adipocyte markers. (**A**) List of the first 45 upregulated genes in 3 samples of SC-WAT of $Egr1^{-/-}$ versus $Egr1^{+/+}$ 2-week-old mice. (**B,C**) RT-qPCR analysis of the expression levels for generic adipocyte differentiation markers

Cebpb, *Ppara*, beige adipocyte differentiation marker, *Ppargc1a*, *Cox8b*, *Cidea, Dio2*, *Pank1, Plin5, Ogdh* and *Sucla2* in SC-WAT of 2-week-old (**B**) and 4-month-old (**C**) *Egr1*$^{-/-}$ mice compared to *Egr1*$^{+/+}$ mice. For each gene, the mRNA levels of control (*Egr1*$^{+/+}$) SC-WAT were normalized to 1. Graphs show means ± standard deviations of 7 samples from 2-week-old *Egr1*$^{+/+}$ mice, 5 samples from 2-week-old *Egr1*$^{-/-}$ mice, and 5 samples from 4-month-old wild type and mutant mice. The p-values were obtained using the Mann-Withney test. Asterisks indicate the p-values * p<0.05, ** p<0.01. (**D**) ChIP assays were performed from 20 fat pads of 2-week-old mice with antibodies against EGR1 or IgG2 as irrelevant antibody in three independent biological experiments. ChIP products were analyzed by RT-q-PCR (N=2). Primers targeting the proximal promoter regions of *Cebpb* and *Ucp1* revealed the recruitment of EGR1 in the vicinity of these sequences, while primers targeting the proximal promoter regions of *Ppargc1a* and *Gapdh* (negative controls) did not show any immunoprecipitation with EGR1 antibody compared to IgG2 antibody. Results were represented as percentage of the input. Error bars showed standard deviations. The p-values were obtained using the Mann-Withney test. Asterisks indicate the p-values, ** p<0.01, *** p<0.001.

Figure 2-figure supplement 1

List of upregulated genes in the inguinal subcutaneous adipose tissue of 2-week-old *Egr1*$^{-/-}$ mice versus wild-type mice.

Figure 2-figure supplement 2

Gene Ontology analysis of the upregulated genes in the inguinal subcutaneous adipose tissue of *Egr1*$^{+/+}$ versus *Egr1*$^{-/-}$ 2-week-old mice using the DAVID Bioinformatics Resources 6.8.

Figure 3. Transcriptomic analysis of the subcutaneous inguinal adipose tissue of postnatal *Egr1*$^{-/-}$ versus *Egr1*$^{+/+}$ mice reveals downregulation of extracellular matrix genes. (**A**) List of downregulated extracellular matrix genes in the inguinal subcutaneous adipose tissue of 2-week-old *Egr1*$^{-/-}$ mice versus wild-type mice. (**B,C**) RT-qPCR analysis of gene expression levels for extracellular matrix genes, *Col1a1, Col5a2, Col14a1, Fn1, Postn, Dcn* and *Mmp2,* in SC-WAT of 2-week-old (**B**) and 4-month-old (**C**) *Egr1*$^{+/+}$ and *Egr1*$^{-/-}$ mice. For each gene, the mRNA levels of control (*Egr1*$^{+/+}$) SC-WAT were normalized to 1. Graphs show means ± standard deviations of 7 samples from 2-week-old *Egr1*$^{+/+}$ mice, 5 samples from 2-week-old *Egr1*$^{-/-}$ mice and 5 samples from 4-month-old wild type and mutant mice. The p-values were obtained using the Mann-Withney test. Asterisks indicate the p-values * p<0.05, ** p<0.01.

Figure 3-figure supplement 1

List of downregulated genes in the inguinal subcutaneous adipose tissue of 2-week-old *Egr1*$^{-/-}$ mice versus wild-type mice.

Figure 3-figure supplement 2

Gene Ontology analysis of downregulated genes in the inguinal subcutaneous adipose tissue of *Egr1*$^{+/+}$ versus *Egr1*$^{-/-}$ 2-week-old mice using the DAVID Bioinformatics Resources 6.8.

Figure 4. *Egr1* gain-of-function decreases beige adipocyte differentiation in mouse mesenchymal stem cells. (**A**) C3H10T1/2 and C3H10T1/2-*Egr1* cells subjected to beige adipocyte differentiation for 8 days were then stained with Oil Red O and Hematoxilin/Eosin at Day 0 (confluence) and Day 8, or immuno-stained with UCP1 antibody and counterstained with Hematoxilin/Eosin at Day 8. Scale bars: Oil red O staining 50μm, UCP1 immunostaining 25μm. (**B**) C3H10T1/2 and C3H10T1/2-Egr1 cell density after 8 days in beige differentiation medium. Graphs show means ± standard deviations of cell number from 10 pictures in each condition. The p-values were obtained using the Mann-Whitney test. Asterisks indicate the p-value **** P<0.0001. (**C**) RT-qPCR analysis of the expression levels for the adipocyte transcriptional activator *Ppara*, the beige markers, *Ucp1*, *Cidea, Plin5, Ogdh,* and the extracellular component *Col5a2* in C3H10T1/2 and C3H10T1/2-*Egr1* cells subjected to beige adipocyte differentiation. For each gene, the mRNA levels of the control C3H10T1/2 cells at Day 0 or from the first day of detection were normalised to 1. *Ogdh* and *Col5a2* expression was detected from Day 0, *Ppara*, *Cidea* and *Plin5* expression was detected from Day 6, *Ucp1* expression was detected at day 8. The graphs show the relative levels of mRNAs in C3H10T1/2 and C3H10T1/2-*Egr1* cells at different time points (Day 0, Day 1, Day 6, and Day 8) of beige adipocyte differentiation compared to C3H10T1/2 cells at Day 0 or to C3H10T1/2 cells from the first day of gene detection. For each time point, graphs show means ± standard deviations of 6 samples. The p values were calculated using the Mann-Withney test. Asterisks indicate the p-values of gene expression levels in C3H10T1/2-*Egr1* cells or C3H10T1/2 cells compared to Day 0 (*Ogdh* and *Col5a2*) or from the first day of gene detection (*Ppara*, *Cidea, Ucp1* and *Plin5)*, **P<0.01. # indicate the p-values of gene expression levels in C3H10T1/2-*Egr1* versus C3H10T1/2 cells, for each time point, ## P<0.01; # P<0.05. (**D**) Schematic cellular location of proteins encoded by *Egr1* regulated genes in SC-WAT. *Egr1* deletion upregulates the expression of genes encoding

proteins involved in the beige adipocyte differentiation network (C/EBPß, PPARγ, PGC1α), thermogenesis (UCP1, COX8B, SUCLA2, OGDH), metabolism (CIDEA, PLIN5, PANK1), or thyroid hormone metabolism (DIO2). *Egr1* is expressed in adipocytes and the encoded protein is recruited to the *Cebpb* and *Ucp1* promoters. This indicates that EGR1 directly represses WAT browning. *Egr1* deletion downregulates the expression of genes encoding extracellular matrix proteins such as Collagens, Fibronectin and Perisotin.

Figure 4-figure supplement 1

***Egr1* gain-of-function decreases white and beige adipose tissue differentiation in mouse mesenchymal stem cells.** (**A**) C3H10T1/2 and C3H10T1/2-*Egr1* cells subjected to white adipocyte differentiation for 10 days were stained with Oil Red O and Hematoxilin/Eosin at Day 0 (confluence) and Day 10, or immuno-stained with UCP1 antibody and counterstained with Hematoxilin/Eosin at Day 10. UCP1 was never found to be expressed in cells cultured in white adipocyte differentiation medium. Scale bars: Oil red O staining 50μm, UCP1 immunostaining 25μm. (**B-E**) RT-qPCR analysis of the expression levels for the generic adipocyte differentiation genes *Cebpb, Pparag, Ppara*, the white differentiation marker *Retn* (**B**), the thermogenic marker *Ucp1* (**C**), the extracellular matrix genes *Col5a2*, *Fn1* and *Postn* (**D**), in C3H10T1/2 and C3H10T1/2-*Egr1* cells subjected to 10 days of white adipocyte differentiation conditions. *Egr1* repressed the expression of *Cepbb*, *Pparg Ppara* and *Retn*, involved in the white adipocyte differentiation program and activated the expression of ECM genes, *Col5a2*, *Fn1* and *Postn* during white adipocyte differentiation. *Ucp1* expression was not detected in cells cultured in white differentiation conditions. (**E**) RT-qPCR analysis of the expression levels for the generic adipocyte differentiation marker *Cebpb*, beige adipocyte markers *Pank1 and Sucla2* and ECM genes *Fn1* and *Postn* in C3H10T1/2 and C3H10T1/2-*Egr1* cells subjected to 8 days of beige adipocyte differentiation. EGR1 repressed the expression of *Cepbb* and the beige adipocyte markers *Pank1 and Sucla2*. EGR1 activated the expression of ECM genes *Col5a2*, *Fn1* and *Postn* during beige adipocyte differentiation. The mRNA levels of the C3H10T1/2 cells at day 0 or from the first day of detection were normalized to 1, so the graphs show the relative levels of mRNA in the C3H10T1/2 (n=6) and C3H10T1/2-*Egr1* cells (n=6) at different time points (Day 0, Day 1, Day 4, and Day 10 of white adipocyte differentiation or Day 0, Day 1, Day 6 and Day 8 of beige adipocyte differentiation) compared to C3H10T1/2 cells at day 0 or from the first day of gene detection. Error bars indicate standard deviations. The p values were calculated using the Mann-Withney test. Asterisks indicate the p-values of gene expression levels in C3H10T1/2-*Egr1* cells or C3H10T1/2 cells compared to Day 0 (*Cebpb, Pparg, Col5a2, Fn1, Postn, Pank1,*

Sucla2) or from the first day of gene detection (*Ppara*, Retn*)*, *** P<0.001, **P<0.01. # indicate the p-values of gene expression levels in C3H10T1/2-*Egr1* versus C3H10T1/2 cells, for each time point, ## P<0.01; # P<0.05.

Supplementary Table 1

List of primers used for quantitative PCR.

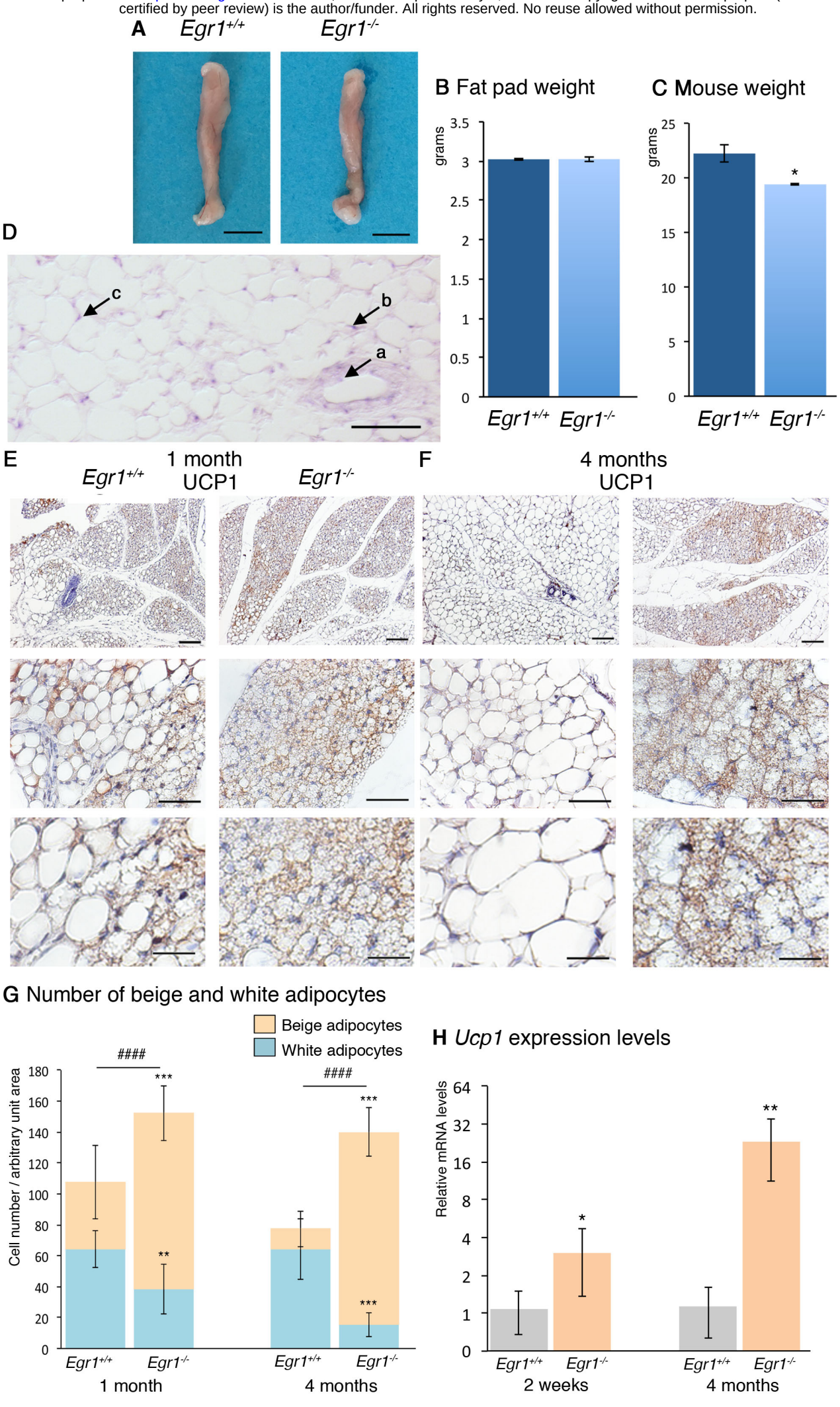

Figure 1

A

Gene symbol	log2(FoldChange)	Fold Change	padj
Dio2	1.421	2.677	4.63E-09
Acot11	1.171	2.251	1.92E-07
Pm20d1	1.052	2.074	2.36E-04
Ucp1	1.050	2.071	1.18E-07
Dhrs9	0.971	1.961	9.52E-04
Ppargc1a	0.870	1.827	6.30E-04
Slc25a42	0.860	1.815	1.26E-06
Cidea	0.818	1.763	6.35E-04
Plin5	0.817	1.762	1.46E-04
Pank1	0.815	1.759	1.97E-04
Cpn2	0.809	1.752	5.18E-03
Dhrs11	0.804	1.746	2.96E-03
Ppargc1b	0.792	1.732	3.45E-04
Kng2	0.785	1.723	8.74E-03
Gpd2	0.783	1.721	5.70E-04
Slc36a2	0.750	1.682	1.70E-04
Otop1	0.748	1.679	8.21E-04
Letmd1	0.747	1.679	1.41E-03
Acacb	0.747	1.679	2.57E-03
Clstn3	0.725	1.653	1.78E-02
Ldhb	0.719	1.646	2.83E-03
Mlxipl	0.706	1.632	3.11E-03
Cox5a	0.694	1.618	2.10E-03
Coq6	0.684	1.607	4.08E-03
Mrap	0.684	1.606	1.42E-03
Ppara	0.682	1.604	9.66E-03
Nampt	0.678	1.600	1.42E-03
Gpd1	0.675	1.596	5.58E-03
Cox8b	0.670	1.591	2.10E-03
Cisd3	0.664	1.584	1.91E-02
Lrg1	0.659	1.579	1.50E-02
Ogdh	0.653	1.572	2.81E-03
Cs	0.645	1.563	3.97E-03
Hadhb	0.642	1.561	5.77E-03
Aco2	0.628	1.546	6.26E-03
Sucla2	0.626	1.543	8.09E-03
Kcnk3	0.625	1.543	1.13E-02
Sh2b2	0.621	1.538	5.44E-03
Cpt1b	0.620	1.537	2.54E-02
Ntrk3	0.619	1.536	8.33E-03
Slc25a22	0.611	1.527	2.35E-02
Apoc1	0.605	1.521	9.48E-03
Idh3a	0.586	1.501	1.02E-02
Cebpb	0.583	1.498	2.03E-02
Mdh2	0.565	1.479	1.62E-02

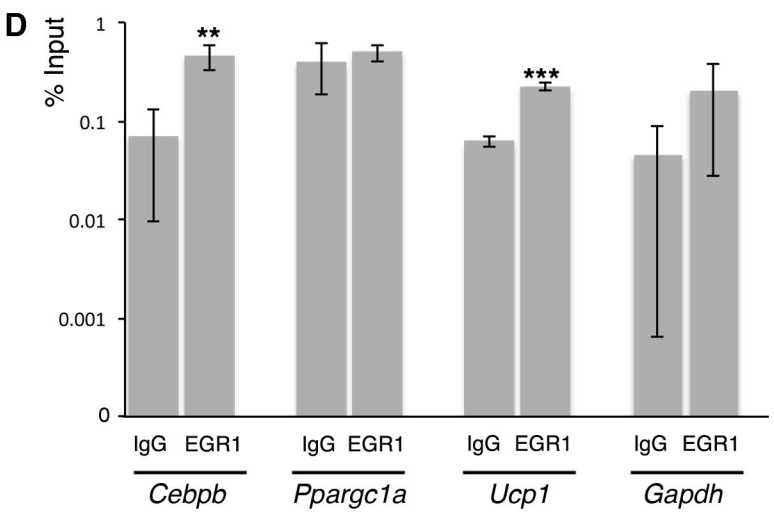

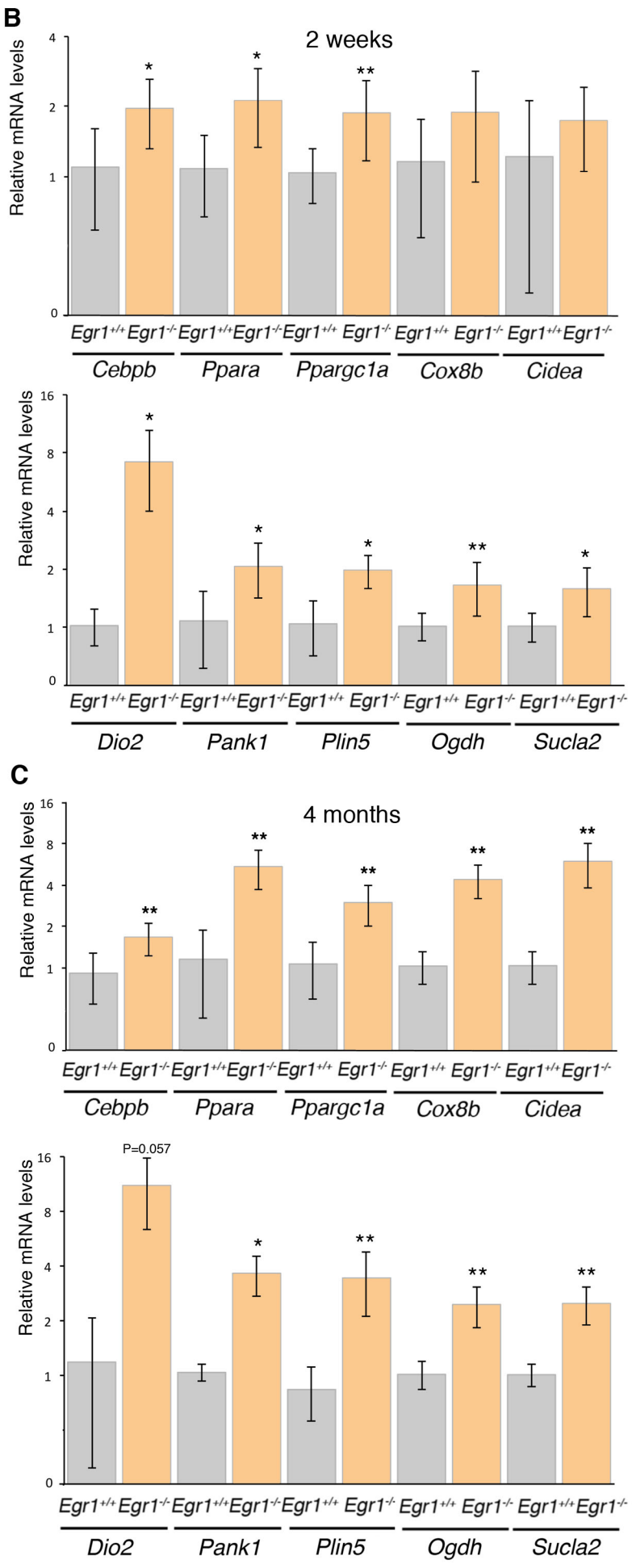

Figure 2

Figure 2-figure supplement 1: List of up-regulated genes in the ingWAT of postnatal Egr1-/- mice

Contig	log2FoldChar	Fold Change	padj	Description
Genes expressed in adipose tissue derived- mesenchymal stem cells				
Gnas	0.471	1.386	3.94E-02	GNAS (guanine nucleotide binding protein, alpha stimulating) complex locus
Genes expressed during adipocytes (white/beige) differentiation				
Cebpb	0.583	1.498	2.03E-02	CCAAT/enhancer binding protein (C/EBP), beta
Ppara	0.682	1.604	9.66E-03	peroxisome proliferator activated receptor alpha
Genes expressed in beige differenciated adipocytes: metabolism and thermogenic genes				
Acacb	0.747	1.679	2.57E-03	acetyl-Coenzyme A carboxylase beta
Acadm	0.508	1.422	3.32E-02	acyl-Coenzyme A dehydrogenase, medium chain
Acadvl	0.504	1.418	3.47E-02	acyl-Coenzyme A dehydrogenase, very long chain
Aco2	0.628	1.546	6.26E-03	aconitase 2, mitochondrial
Acot11	1.171	2.251	1.92E-07	acyl-CoA thioesterase 11
Apoc1	0.605	1.521	9.48E-03	apolipoprotein C-I
bscl2	0.479	1.394	2.18E-02	BSCL2, seipin lipid droplet biogenesis associated
Chchd10	0.502	1.416	4.64E-02	coiled-coil-helix-coiled-coil-helix domain containing 10
Cidea	0.818	1.763	6.35E-04	cell death-inducing DNA fragmentation factor, alpha subunit-like effector A
Cisd3	0.664	1.584	1.91E-02	CDGSH iron sulfur domain 3
Clstn3	0.725	1.653	1.78E-02	calsyntenin 3
Cluh	0.552	1.466	1.01E-02	clustered mitochondria (cluA/CLU1) homolog
Coq6	0.684	1.607	4.08E-03	coenzyme Q6 monooxygenase
Cox5a	0.694	1.618	2.10E-03	cytochrome c oxidase subunit Va
Cox8b	0.670	1.591	2.10E-03	cytochrome c oxidase subunit VIIIb
Cpn2	0.809	1.752	5.18E-03	carboxypeptidase N, polypeptide 2
Cpt1b	0.620	1.537	2.54E-02	carnitine palmitoyltransferase 1b, muscle
Cs	0.645	1.563	3.97E-03	citrate synthase] [Gene Type: protein-coding]
Cspg4	0.563	1.478	2.63E-02	chondroitin sulfate proteoglycan 4
Cyc1	0.486	1.401	4.44E-02	cytochrome c-1
Dhrs11	0.804	1.746	2.96E-03	dehydrogenase/reductase (SDR family) member 11

Dhrs9	0.971	1.961	9.52E-04	dehydrogenase/reductase (SDR family) member 9
Dio2	1.421	2.677	4.63E-09	deiodinase, iodothyronine, type II
Elovl6	0.536	1.450	4.30E-02	ELOVL family member 6, elongation of long chain fatty acids (yeast)]
Etfa	0.525	1.439	2.03E-02	electron transferring flavoprotein, alpha polypeptide
Etfdh	0.506	1.420	3.34E-02	electron transferring flavoprotein, dehydrogenase
Gpd1	0.675	1.596	5.58E-03	glycerol-3-phosphate dehydrogenase 1 (soluble)
Gpd2	0.783	1.721	5.70E-04	glycerol phosphate dehydrogenase 2, mitochondrial
Hadhb	0.642	1.561	5.77E-03	hydroxyacyl-Coenzyme A dehydrogenase, beta subunit
Idh3a	0.586	1.501	1.02E-02	isocitrate dehydrogenase 3 (NAD+) alpha
Idh3g	0.497	1.411	2.36E-02	isocitrate dehydrogenase 3 (NAD+), gamma
Kcnk3	0.625	1.543	1.13E-02	potassium channel, subfamily K, member 3
Kng2	0.785	1.723	8.74E-03	kininogen 2
Ldhb	0.719	1.646	2.83E-03	lactate dehydrogenase B
Letmd1	0.747	1.679	1.41E-03	LETM1 domain containing 1
Lrg1	0.659	1.579	1.50E-02	leucine-rich alpha-2-glycoprotein 1
Mdh2	0.565	1.479	1.62E-02	malate dehydrogenase 2, NAD (mitochondrial)
Mecr	0.547	1.461	1.04E-02	mitochondrial trans-2-enoyl-CoA reductase
Mlxipl	0.706	1.632	3.11E-03	MLX interacting protein-like
Mrap	0.684	1.606	1.42E-03	melanocortin 2 receptor accessory protein
Nampt	0.678	1.600	1.42E-03	nicotinamide phosphoribosyltransferase
Nrg4	0.454	1.370	2.75E-02	neuregulin 4
Ntrk3	0.619	1.536	8.33E-03	neurotrophic tyrosine kinase, receptor, type 3
Nudt7	0.494	1.409	4.56E-02	nudix (nucleoside diphosphate linked moiety X)-type motif 7
Ogdh	0.653	1.572	2.81E-03	oxoglutarate (alpha-ketoglutarate) dehydrogenase (lipoamide)
Oplah	0.563	1.477	7.75E-03	5-oxoprolinase (ATP-hydrolysing)
Otop1	0.748	1.679	8.21E-04	otopetrin 1
Pald1	0.491	1.405	2.54E-02	phosphatase domain containing, paladin 1
Pank1	0.815	1.759	1.97E-04	pantothenate kinase 1
Plin5	0.817	1.762	1.46E-04	perilipin 5
Pm20d1	1.052	2.074	2.36E-04	peptidase M20 domain containing 1
Ppargc1a	0.870	1.827	6.30E-04	peroxisome proliferative activated receptor, gamma, coactivator 1 alpha
Ppargc1b	0.792	1.732	3.45E-04	peroxisome proliferative activated receptor, gamma, coactivator 1 beta

Ptp4a1	0.445	1.362	3.55E-02	protein tyrosine phosphatase 4a1
Sh2b2	0.621	1.538	5.44E-03	SH2B adaptor protein 2
Slc25a20	0.540	1.454	3.06E-02	solute carrier family 25 (mitochondrial carnitine/acylcarnitine translocase), member 20
Slc25a22	0.611	1.527	2.35E-02	solute carrier family 25 (mitochondrial carrier, glutamate), member 22
Slc25a42	0.860	1.815	1.26E-06	solute carrier family 25, member 42
Slc25a51	0.539	1.453	8.47E-03	solute carrier family 25, member 51
Slc36a2	0.750	1.682	1.70E-04	solute carrier family 36 (proton/amino acid symporter), member 2
Slc4a4	0.490	1.404	6.12E-03	solute carrier family 4 (anion exchanger), member 4
Sucla2	0.626	1.543	8.09E-03	succinate-Coenzyme A ligase, ADP-forming, beta subunit
Suclg1	0.541	1.455	2.33E-02	succinate-CoA ligase, GDP-forming, alpha subunit]
Ucp1	1.050	2.071	1.18E-07	uncoupling protein 1 (mitochondrial, proton carrier)

Genes expressed in White adipose metabolism

Adra1a	1.056	2.079	2.95E-08	adrenergic receptor, alpha 1a
Adrbk2	0.641	1.559	4.79E-03	adrenergic, beta, receptor kinase 2
Chst3	0.588	1.503	4.61E-02	carbohydrate (chondroitin 6/keratan) sulfotransferase 3
Cmtm4	0.550	1.464	1.84E-02	CKLF-like MARVEL transmembrane domain containing 4
Cntfr	0.723	1.651	2.22E-02	ciliary neurotrophic factor receptor
Cntnap1	0.656	1.576	4.44E-02	contactin associated protein-like 1
Crat	0.504	1.418	1.90E-02	carnitine acetyltransferase
Ctse	1.659	3.157	2.07E-10	cathepsin E
Dcun1d3	0.512	1.426	4.08E-02	DCN1, defective in cullin neddylation 1, domain containing 3
Dgat2	0.647	1.566	1.19E-02	diacylglycerol O-acyltransferase 2
Gk	1.074	2.106	1.74E-09	glycerol kinase
Gys1	0.553	1.468	1.97E-02	glycogen synthase 1, muscle
Helz2	0.518	1.432	1.97E-02	helicase with zinc finger 2, transcriptional coactivator
Hk2	0.804	1.746	3.42E-04	hexokinase 2
Mif4gd	0.509	1.423	3.01E-02	MIF4G domain containing/serum leptin-interacting protein 1
Pdp2	0.583	1.498	2.75E-02	pyruvate dehyrogenase phosphatase catalytic subunit 2
Pnpla3	0.819	1.764	6.72E-04	patatin-like phospholipase domain containing 3
Ppip5k1	0.531	1.445	2.06E-02	diphosphoinositol pentakisphosphate kinase 1
Ppp1r10	0.462	1.377	4.01E-02	protein phosphatase 1, regulatory subunit 10

Rtn4ip1	0.531	1.445	4.47E-02	reticulon 4 interacting protein 1
Syt12	0.777	1.714	1.13E-02	synaptotagmin XII
Tfrc	1.189	2.280	1.18E-07	transferrin receptor
Tysnd1	0.553	1.467	4.20E-02	trypsin domain containing 1

Genes involved in inflammation in adipose tissue

Cdkn1a	0.654	1.574	3.55E-02	cyclin-dependent kinase inhibitor 1A (P21)
Ifit1	0.795	1.735	2.54E-02	interferon-induced protein with tetratricopeptide repeats 1
Il15ra	0.483	1.398	3.95E-02	interleukin 15 receptor, alpha chain
Il2rb	0.810	1.753	1.43E-02	interleukin 2 receptor, beta chain
Irf7	0.702	1.626	2.54E-02	interferon regulatory factor 7
Tmem38b	0.501	1.415	4.29E-02	transmembrane protein 38B
Tob1	0.524	1.438	5.25E-03	transducer of ErbB-2.1
Tob2	0.698	1.623	2.79E-03	transducer of ERBB2, 2
Traf4	0.591	1.506	4.93E-02	TNF receptor associated factor 4
Usp2	0.642	1.560	2.59E-02	ubiquitin specific peptidase 2

Genes expressed in other cell types within the adipose tissue

Adam11	0.633	1.550	2.79E-02	a disintegrin and metallopeptidase domain 11
Bst2	0.705	1.630	3.55E-02	bone marrow stromal cell antigen 2
Cnnm2	0.614	1.530	4.39E-02	cyclin M2
Cd79a	0.672	1.594	4.61E-02	CD79A antigen
Cdh2	0.611	1.527	1.73E-02	cadherin 2
Csrnp1	0.715	1.641	2.05E-02	cysteine-serine-rich nuclear protein 1
Dlat	0.505	1.419	3.96E-02	dihydrolipoamide S-acetyltransferase (E2 component of pyruvate dehydrogenase complex)
Dlst	0.510	1.424	2.62E-02	dihydrolipoamide S-succinyltransferase (E2 component of 2-oxo-glutarate complex)
Fggy	0.717	1.644	1.35E-02	FGGY carbohydrate kinase domain containing
Gramd1b	0.566	1.480	1.40E-02	GRAM domain containing 1B
Pax5	0.687	1.610	3.11E-02	paired box 5
Perm1	0.712	1.638	1.05E-02	PPARGC1 and ESRR induced regulator, muscle 1
Sbk1	0.594	1.509	1.13E-02	SH3-binding kinase 1
Sec61a2	0.536	1.450	1.90E-02	Sec61, alpha subunit 2 (S. cerevisiae)

Trim67	1.374	2.591	2.58E-11	tripartite motif-containing 67

Genes with unidentified function or Non coding RNA

1110001J03Rik	0.744	1.675	5.77E-03	
Ctcflos	0.673	1.594	3.80E-03	CCCTC-binding factor (zinc finger protein)-like, opposite strand (ncRNA)
Fam126b	0.440	1.357	2.16E-02	family with sequence similarity 126, member B
Fam210a	0.507	1.422	2.96E-02	family with sequence similarity 210, member A
Fam73b	0.689	1.613	1.32E-03	family with sequence similarity 210, member A
Gdap10	0.950	1.932	8.41E-07	ganglioside-induced differentiation-associated-protein 10 (ncRNA)
Gm10032	0.754	1.686	3.59E-02	predicted gene 10032 (ncRNA)
Gm37674	0.680	1.603	3.98E-02	-
Gm37783	0.725	1.653	2.14E-02	-
Gm38357	0.680	1.602	1.22E-02	-
Gm42428	0.765	1.699	1.23E-02	-
Gm42614	0.944	1.924	1.42E-03	-
Gm42895	0.741	1.671	2.52E-02	-
Gm43605	0.772	1.707	2.14E-02	-
Gm8822	2.452	5.473	5.82E-23	ARP3 actin-related protein 3 homolog pseudogene
Gm9899	0.668	1.589	1.98E-02	predicted gene 9899 (ncRNA)
RP23-82I13.6	0.813	1.757	1.34E-03	-

GOTERM_BP_DIRECT	**Up regulated genes in the inguinal subcutaneous adipose tissue of 2-week-old *Egr1*$^{-/-}$ mice**	
	Enrichment scores / P-values	**Genes**
NADH Metabolic process	**95.2**/ 3.3^{E}-11	*Dlst* dihydrolipoamide S-succinyltransferase *Gpd2* glycerol phosphate dehydrogenase 2, mitochondrial *Gpd1* glycerol-3-phosphate dehydrogenase 1 (soluble) *Idh3a* isocitrate dehydrogenase 3 (NAD+) alpha *Idh3g* isocitrate dehydrogenase 3 (NAD+), gamma *Mdh2* malate dehydrogenase 2, NAD (mitochondrial) *Ogdh* oxoglutarate (alpha-ketoglutarate) dehydrogenase
Tricarboxylic acid cycle	**53.4**/ 1.1^{E}-13	*Aco2* aconitase 2, mitochondrial *Cs* citrate synthase *Dlat* dihydrolipoamide S-acetyltransferase *Dlst* dihydrolipoamide S-succinyltransferase *Idh3a* isocitrate dehydrogenase 3 (NAD+) alpha *Idh3g* isocitrate dehydrogenase 3 (NAD+), gamma *Mdh2* malate dehydrogenase 2, NAD (mitochondrial) *Ogdh* oxoglutarate (alpha-ketoglutarate) dehydrogenase *Suclg1* succinate-CoA ligase, GDP-forming, alpha subunit *Sucla2* succinate-Coenzyme A ligase, ADP-forming, beta subunit
Brown fat cell differentiation	**23.4** /5.7^{E}-5	*Cebpb* CCAAT/enhancer binding protein (C/EBP), beta *Sh2b2* SH2B adaptor protein 2 *Lrg1* leucine-rich alpha-2-glycoprotein 1 *Mrap* melanocortin 2 receptor accessory protein *Nudt7* nudix -type motif 7 *Ucp1* uncoupling protein 1
Fatty acid metabolic process	**9.9** /7.1^{E}-7	*Elovl6* elongation of long chain fatty acids, member 6 *Acacb* acetyl-Coenzyme A carboxylase beta *Acot11* acyl-CoA thioesterase 11 *Acadm* acyl-Coenzyme A dehydrogenase, medium chain

		Acadvl acyl-Coenzyme A dehydrogenase, very long chain *Crat* carnitine acetyltransferase *Cpt1b* carnitine palmitoyltransferase 1b *Hadhb* hydroxyacyl-Coenzyme A dehydrogenase *Mecr* mitochondrial trans-2-enoyl-CoA reductase *Ppara* peroxisome proliferator activated receptor alpha
Metabolic process	**4.9**/ 6 .9^{E}-7	*Acacb* acetyl-Coenzyme A carboxylase beta *Aco2* aconitase 2, mitochondrial *Acadm* acyl-Coenzyme A dehydrogenase, medium chain *Acadvl* acyl-Coenzyme A dehydrogenase, very long chain *Dhrs11* dehydrogenase/reductase (SDR family) member 11 *Dhrs9* dehydrogenase/reductase (SDR family) member 9 *Dlat* dihydrolipoamide S-acetyltransferase *Dlst* dihydrolipoamide S-succinyltransferase *Gys1* glycogen synthase 1, muscle *Hk2* hexokinase 2 Hadhb hydroxyacyl-Coenzyme A dehydrogenase Ogdh oxoglutarate (alpha-ketoglutarate) dehydrogenase Pnpla3 patatin-like phospholipase domain containing 3 Pm20d1 peptidase M20 domain containing 1 Suclg1 succinate-CoA ligase, GDP-forming, alpha subunit) Sucla2 succinate-Coenzyme A ligase, ADP-forming, beta subunit
Lipid metabolic process	**4.7** /8.3^{E}-6	Bscl2 Berardinelli-Seip congenital lipodystrophy 2 Elovl6 elongation of long chain fatty acids, member 6 Acacb acetyl-Coenzyme A carboxylase beta Acadm acyl-Coenzyme A dehydrogenase, medium chain Acadvl acyl-Coenzyme A dehydrogenase, very long chain) Crat carnitine acetyltransferase Cpt1b carnitine palmitoyltransferase 1b Cidea cell death-inducing DNA fragmentation factor, alpha subunit-like effector A Dgat2 diacylglycerol O-acyltransferase 2

		Hadhb hydroxyacyl-Coenzyme A dehydrogenase Mecr mitochondrial trans-2-enoyl-CoA reductase Pnpla3 patatin-like phospholipase domain containing 3 Plin5 perilipin 5 Ppara peroxisome proliferator activated receptor alpha

Figure 2-figure supplement 2

A

Gene symbol	Log2 (Fold Change)	Fold Change	Padj
Srpx2	-0.799	0.575	1.77E-03
Dcn	-0.790	0.578	7.84E-06
Fbn1	-0.781	0.582	7.58E-05
Pcolce2	-0.771	0.586	4.73E-03
Pcdhb14	-0.749	0.595	5.51E-03
Lum	-0.741	0.598	1.50E-05
Efemp1	-0.735	0.601	1.15E-03
Aspn	-0.698	0.616	1.64E-03
Pcdh20	-0.697	0.617	2.37E-02
Col14a1	-0.692	0.619	2.01E-05
Fn1	-0.676	0.626	2.04E-04
Dpysl3	-0.669	0.629	1.08E-03
Tppp3	-0.667	0.630	1.26E-02
Vnn3	-0.663	0.632	1.94E-02
Vcan	-0.646	0.639	1.13E-02
Dpt	-0.641	0.641	4.05E-03
Mmp23	-0.630	0.646	8.69E-03
Adgre1	-0.622	0.650	1.23E-02
Adgrd1	-0.617	0.652	3.91E-02
Postn	-0.615	0.653	1.21E-03
Itgbl1	-0.604	0.658	4.20E-02
Fap	-0.600	0.660	4.05E-03
Col5a2	-0.598	0.661	1.95E-03
Dbn1	-0.598	0.661	4.64E-02
Thbs3	-0.575	0.671	2.05E-02
Adamtsl4	-0.557	0.680	4.61E-02
Cdh11	-0.555	0.681	3.46E-02
Dab2	-0.555	0.681	1.76E-02
Ckap4	-0.552	0.682	2.14E-02
Col3a1	-0.549	0.684	6.47E-03
Col1a1	-0.549	0.684	8.29E-03
Ddr2	-0.548	0.684	7.24E-03
Ecm2	-0.541	0.688	3.83E-02
Timp2	-0.537	0.689	2.54E-02
Fndc1	-0.535	0.690	4.21E-02
Col1a2	-0.522	0.696	8.78E-03
Antxr1	-0.520	0.697	1.51E-02
Apcdd1	-0.517	0.699	4.18E-02
Fmr1	-0.504	0.705	2.61E-02
Adamts2	-0.488	0.713	3.83E-02
Mmp14	-0.478	0.718	3.95E-02
Mmp2	-0.464	0.725	3.66E-02

B

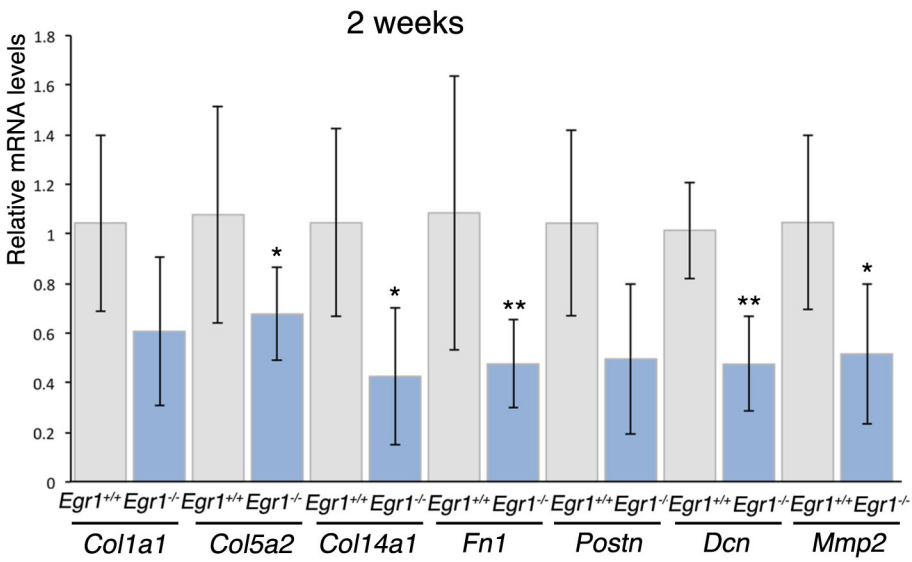

C

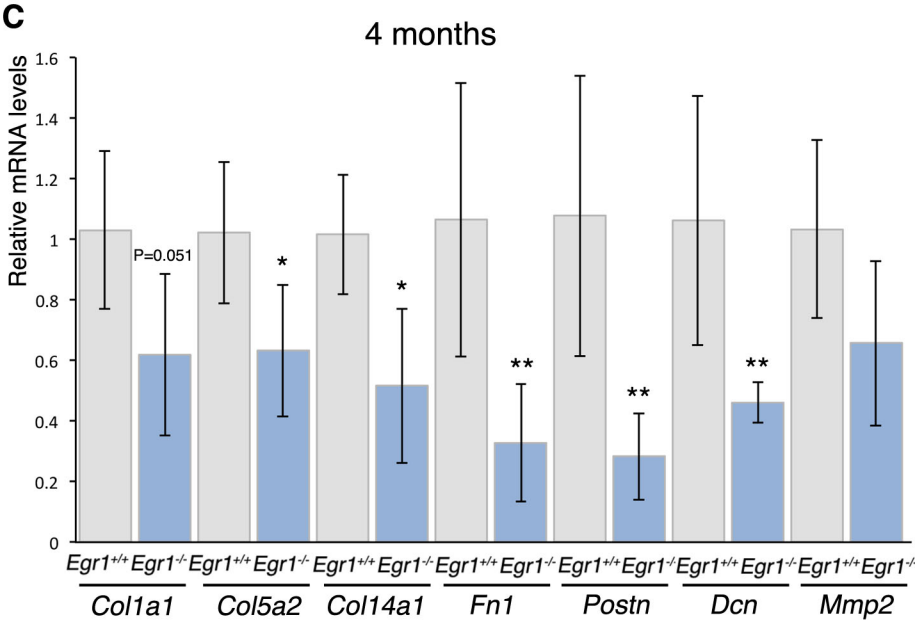

Figure 3

Figure 3-figure supplement 1: List of down-regulated genes in the ingWAT of postnatal Egr1-/- mice

Gene symbol	Log2 (Fold Cł	Fold Change	padj	Description
Extracellular matrix, cytoskeleton and adhesion genes				
Adamts2	-0.488	0.713	3.83E-02	a disintegrin-like and metallopeptidase (reprolysin type) with thrombospondin type 1 motif, 2
Adamtsl4	-0.557	0.680	4.61E-02	ADAMTS-like 4
Adgrd1	-0.617	0.652	3.91E-02	adhesion G protein-coupled receptor D1
Adgre1	-0.622	0.650	1.23E-02	adhesion G protein-coupled receptor E1
Antxr1	-0.520	0.697	1.51E-02	anthrax toxin receptor 1
Aspn	-0.698	0.616	1.64E-03	asporin
Apcdd1	-0.517	0.699	4.18E-02	adenomatosis polyposis coli down-regulated 1
Cdh11	-0.555	0.681	3.46E-02	cadherin 11
Ckap4	-0.552	0.682	2.14E-02	cytoskeleton-associated protein 4
Col14a1	-0.692	0.619	2.01E-05	collagen, type XIV, alpha 1
Col1a1	-0.549	0.684	8.29E-03	collagen, type I, alpha 1
Col1a2	-0.522	0.696	8.78E-03	collagen, type I, alpha 2
Col3a1	-0.549	0.684	6.47E-03	collagen, type III, alpha 1
Col5a2	-0.598	0.661	1.95E-03	collagen, type V, alpha 2
Dab2	-0.555	0.681	1.76E-02	disabled 2, mitogen-responsive phosphoprotein
Dbn1	-0.598	0.661	4.64E-02	drebrin 1
Dcn	-0.790	0.578	7.84E-06	decorin
Ddr2	-0.548	0.684	7.24E-03	discoidin domain receptor family, member 2
Dpt	-0.641	0.641	4.05E-03	dermatopontin
Dpysl3	-0.669	0.629	1.08E-03	dihydropyrimidinase-like 3
Ecm2	-0.541	0.688	3.83E-02	extracellular matrix protein 2, female organ and adipocyte specific
Efemp1	-0.735	0.601	1.15E-03	epidermal growth factor-containing fibulin-like extracellular matrix protein 1
Fap	-0.600	0.660	4.05E-03	fibroblast activation protein
Fbn1	-0.781	0.582	7.58E-05	fibrillin 1
Fmr1	-0.504	0.705	2.61E-02	fragile X mental retardation syndrome 1
Fn1	-0.676	0.626	2.04E-04	fibronectin 1
Fndc1	-0.535	0.690	4.21E-02	fibronectin type III domain containing 1
Itgbl1	-0.604	0.658	4.20E-02	integrin, beta-like 1

Lum	-0.741	0.598	1.50E-05	lumican
Mmp14	-0.478	0.718	3.95E-02	matrix metallopeptidase 14 (membrane-inserted)
Mmp2	-0.464	0.725	3.66E-02	matrix metallopeptidase 2]
Mmp23	-0.630	0.646	8.69E-03	matrix metallopeptidase 23
Pcdh20	-0.697	0.617	2.37E-02	protocadherin 20
Pcdhb14	-0.749	0.595	5.51E-03	protocadherin beta 14
Pcolce2	-0.771	0.586	4.73E-03	procollagen C-endopeptidase enhancer 2
Postn	-0.615	0.653	1.21E-03	periostin, osteoblast specific factor
Srpx2	-0.799	0.575	1.77E-03	sushi-repeat-containing protein, X-linked 2
Thbs3	-0.575	0.671	2.05E-02	thrombospondin 3
Timp2	-0.537	0.689	2.54E-02	tissue inhibitor of metalloproteinase 2
Tppp3	-0.667	0.630	1.26E-02	tubulin polymerization-promoting protein family member 3
Vcan	-0.646	0.639	1.13E-02	versican
Vnn3	-0.663	0.632	1.94E-02	vanin 3

Genes involved in adipose tissue metabolism and adipocyte metabolism (cell signalling/cell cycle/transcription)

Aebp1	-0.710	0.611	2.34E-04	Adipocyte Enhancer binding protein 1
Akr1c14	-0.858	0.552	8.06E-04	aldo-keto reductase family 1, member C14
Akr1c18	-0.921	0.528	1.21E-04	aldo-keto reductase family 1, member C18
Alb	-0.734	0.601	3.66E-03	albumin
Aldh1a3	-0.752	0.594	2.10E-03	aldehyde dehydrogenase family 1, subfamily A3
Atp2b4	-0.494	0.710	2.54E-02	ATPase, Ca++ transporting, plasma membrane 4
Atpif1	-0.513	0.701	1.98E-02	ATPase inhibitory factor 1
Casp1	-0.667	0.630	3.32E-02	caspase 1
Ces1f	-0.635	0.644	2.05E-03	Carboxylesterase 1F
Clec3b	-0.711	0.611	8.48E-03	C-type lectin domain family 3, member b
Cyb5r3	-0.659	0.633	3.79E-03	cytochrome b5 reductase 3
Cygb	-0.532	0.692	2.01E-02	cytoglobin
Dnm1	-0.633	0.645	8.04E-03	dynamin 1
Gas7	-0.735	0.601	1.91E-04	growth arrest specific 7
Gatm	-0.537	0.689	3.59E-02	glycine amidinotransferase (L-arginine:glycine amidinotransferase)
Ggh	-0.605	0.658	4.70E-03	gamma-glutamyl hydrolase

Ghr	-0.596	0.662	3.79E-03	growth hormone receptor
Glb1l2	-0.507	0.704	4.59E-03	galactosidase, beta 1-like 2
Gnai1	-0.472	0.721	3.65E-02	guanine nucleotide binding protein (G protein), alpha inhibiting 1
Gpc3	-0.487	0.714	3.25E-02	glypican 3
Gulp1	-0.528	0.693	3.52E-02	GULP, engulfment adaptor PTB domain containing 1]
Hmgn3	-0.683	0.623	1.97E-02	high mobility group nucleosomal binding domain 3
Kdelr3	-0.670	0.629	1.56E-02	KDEL (Lys-Asp-Glu-Leu) endoplasmic reticulum protein retention receptor 3
Klf14	-1.097	0.468	2.34E-04	Kruppel-like factor 14
Klhl13	-0.755	0.592	2.40E-04	kelch-like 13
Lpar1	-0.578	0.670	4.70E-03	lysophosphatidic acid receptor 1
Lrrc17	-0.727	0.604	4.94E-04	leucine rich repeat containing 17
Lrrn4cl	-0.752	0.594	1.56E-03	LRRN4 C-terminal like
Mcm6	-0.593	0.663	1.50E-02	minichromosome maintenance complex component 6
Mfap2	-0.841	0.558	3.58E-03	microfibrillar-associated protein 2
Mfap4	-0.832	0.562	1.69E-03	microfibrillar-associated protein 4
Morf4l2	-0.480	0.717	2.85E-02	mortality factor 4 like 2
Mpz	-0.558	0.679	3.91E-02	myelin protein zero
Mrc1	-0.615	0.653	3.79E-03	mannose receptor, C type 1
Mrc2	-0.484	0.715	3.23E-02	mannose receptor, C type 2
Nr5a2	-0.721	0.607	2.01E-02	nuclear receptor subfamily 5, group A, member 2
Nrk	-0.733	0.601	3.11E-03	Nik related kinase
Nxnl1	-0.757	0.592	2.05E-02	nucleoredoxin-like 1
Olfml1	-0.746	0.596	2.38E-03	olfactomedin-like 1
Olfml2b	-0.654	0.636	1.57E-02	olfactomedin-like 2B
Opcml	-0.716	0.609	5.75E-03	opioid binding protein/cell adhesion molecule-like
P4hb	-0.433	0.741	2.22E-02	prolyl 4-hydroxylase, beta polypeptide
Palm	-0.509	0.703	4.28E-02	paralemmin
Peg10	-0.696	0.617	2.35E-02	paternally expressed 10
Pi15	-0.614	0.653	5.75E-03	peptidase inhibitor 15
Pi16	-0.632	0.645	2.98E-02	peptidase inhibitor 16
Plekha4	-0.746	0.596	8.18E-04	pleckstrin homology domain containing, family A (phosphoinositide binding specific) member 4
Plscr4	-0.743	0.598	5.77E-03	phospholipid scramblase 4

Plxdc2	-0.624	0.649	5.96E-04	plexin domain containing 2
Ptgfrn	-0.761	0.590	1.12E-04	prostaglandin F2 receptor negative regulator
Qpct	-0.739	0.599	2.36E-03	glutaminyl-peptide cyclotransferase (glutaminyl cyclase)
Rab3il1	-0.556	0.680	4.84E-02	RAB3A interacting protein (rabin3)-like 1
Rab7b	-0.763	0.589	2.10E-03	RAB7B, member RAS oncogene family
Rassf8	-0.441	0.737	3.24E-02	Ras association (RalGDS/AF-6) domain family (N-terminal) member 8
Rcan2	-0.716	0.609	7.24E-03	regulator of calcineurin 2
Rcn1	-0.567	0.675	2.99E-03	reticulocalbin 1
Rcn3	-0.582	0.668	3.00E-02	reticulocalbin 3, EF-hand calcium binding domain
Rnase4	-0.589	0.665	2.81E-02	ribonuclease, RNase A family 4
S100a10	-0.487	0.714	3.46E-02	S100 calcium binding protein A10 (calpactin)
S100a6	-0.584	0.667	2.54E-02	S100 calcium binding protein A6 (calcyclin)
Scara5	-0.585	0.667	1.97E-02	scavenger receptor class A, member 5
Sh3d19	-0.509	0.703	2.47E-02	SH3 domain protein D19
Slc5a3	-0.692	0.619	5.61E-03	solute carrier family 5 (inositol transporters), member 3
Smarca1	-0.685	0.622	1.61E-02	SWI/SNF related, matrix associated, actin dependent regulator of chromatin, subfamily a, m1
Sncg	-0.889	0.540	1.12E-04	synuclein, gamma
Srpx2	-0.799	0.575	1.77E-03	sushi-repeat-containing protein, X-linked 2
Tceal8	-0.585	0.667	7.35E-03	transcription elongation factor A (SII)-like 8
Tmeff2	-0.610	0.655	2.47E-02	transmembrane protein with EGF-like and two follistatin-like domains 2
Tmem100	-0.969	0.511	1.29E-04	transmembrane protein 100
Tpsb2	-0.691	0.620	4.72E-02	tryptase beta 2
Ugdh	-0.575	0.672	1.23E-02	UDP-glucose dehydrogenase
Ugt8a	-0.662	0.632	6.15E-03	UDP galactosyltransferase 8A

Genes involved in adipocytes differentiation

Ahnak2	-0.684	0.623	2.46E-03	AHNAK nucleoprotein 2
Arhgef25	-0.561	0.678	2.33E-02	Rho guanine nucleotide exchange factor (GEF) 25
Camk2n1	-0.589	0.665	4.21E-02	calcium/calmodulin-dependent protein kinase II inhibitor 1
Cdkn1c	-0.592	0.663	4.51E-03	cyclin-dependent kinase inhibitor 1C (P57)
Ctsk	-0.636	0.643	7.85E-03	cathepsin K
Ctsl	-0.434	0.740	3.01E-02	cathepsin L

Eid1	-0.489	0.712	3.65E-02	EP300 interacting inhibitor of differentiation 1
Ffar2	-0.624	0.649	6.28E-03	free fatty acid receptor 2
Medag	-0.615	0.653	1.13E-02	mesenteric estrogen dependent adipogenesis
Pros1	-0.448	0.733	4.44E-02	protein S (alpha)
Prrx1	-0.492	0.711	3.04E-02	paired related homeobox 1

Genes involved in inflammation, immune response or expressed in blood cells

Aif1l	-0.665	0.631	1.88E-02	allograft inflammatory factor 1-like
Akap12	-0.681	0.624	2.79E-03	A kinase (PRKA) anchor protein (gravin) 12
Alcam	-0.513	0.701	1.62E-02	activated leukocyte cell adhesion molecule
Anxa1	-0.603	0.658	1.58E-02	annexin A1
Anxa3	-0.505	0.704	2.75E-02	annexin A3
C1qtnf7	-0.767	0.588	5.88E-03	C1q and tumor necrosis factor related protein 7
C3ar1	-0.611	0.655	2.59E-02	complement component 3a receptor 1
Car8	-0.700	0.616	6.74E-03	carbonic anhydrase 8
Cd209f	-0.825	0.564	2.79E-03	CD209f antigen
Cd248	-0.839	0.559	3.42E-04	CD248 antigen, endosialin
Cd34	-0.625	0.649	3.35E-03	CD34 antigen
Cfh	-0.825	0.565	3.42E-04	complement component factor h
Cma1	-0.744	0.597	7.75E-03	chymase 1, mast cell
Commd1	-0.559	0.679	3.57E-02	COMM domain containing 1
Cp	-0.748	0.596	1.36E-03	ceruloplasmin
Cpa3	-0.626	0.648	3.68E-02	carboxypeptidase A3, mast cell
Dse	-0.548	0.684	1.50E-02	dermatan sulfate epimerase
Efhd1	-0.704	0.614	1.19E-02	EF hand domain containing 1
Emilin2	-0.609	0.656	2.00E-02	elastin microfibril interfacer 2
F13a1	-0.695	0.618	4.99E-03	coagulation factor XIII, A1 subunit
Fcgr3	-0.626	0.648	2.01E-02	Fc receptor, IgG, low affinity III
Fcrls	-0.786	0.580	1.13E-02	Fc receptor-like S, scavenger receptor]
Folr2	-0.812	0.570	6.29E-03	folate receptor 2 (fetal)
Frmd4b	-0.498	0.708	3.51E-02	FERM domain containing 4B]
Hba-a1	-0.694	0.618	9.93E-03	hemoglobin alpha, adult chain 1

Il1rl2	-0.549	0.683	3.59E-02	interleukin 1 receptor-like 2
Mal	-0.582	0.668	4.44E-02	myelin and lymphocyte protein, T cell differentiation protein
Morc4	-0.619	0.651	2.11E-02	microrchidia 4
Pf4	-0.730	0.603	6.34E-03	platelet factor 4
Plat	-0.716	0.609	2.10E-03	plasminogen activator, tissue
Ppic	-0.551	0.682	1.46E-02	peptidylprolyl isomerase C
Prnp	-0.468	0.723	3.47E-02	prion protein
Serpinb6a	-0.684	0.622	5.76E-04	serine (or cysteine) peptidase inhibitor, clade B, member 6a
Serpinf1	-0.556	0.680	1.43E-02	serine (or cysteine) peptidase inhibitor, clade F, member 1
Sulf1	-0.532	0.692	1.61E-02	sulfatase 1
Wbp5	-0.683	0.623	2.34E-04	WW domain binding protein 5

Genes encoding secreted molecules

Bmp3	-0.633	0.645	4.01E-02	bone morphogenetic protein 3
Ccdc80	-0.849	0.555	1.09E-04	coiled-coil domain containing 80
Chrdl1	-0.891	0.539	1.20E-04	chordin-like 1
Crispld1	-0.709	0.612	6.15E-03	cysteine-rich secretory protein LCCL domain containing 1
Fgf2	-0.576	0.671	1.56E-02	fibroblast growth factor 2
Fstl1	-0.762	0.590	1.73E-04	follistatin-like 1
Igf1	-0.710	0.611	2.04E-04	insulin-like growth factor 1
Igf2	-0.719	0.608	1.08E-03	insulin-like growth factor 2
Igfbp5	-0.511	0.702	2.00E-02	insulin-like growth factor binding protein 5
Igfbp6	-0.777	0.583	5.58E-03	insulin-like growth factor binding protein 6
Lep	-0.507	0.704	2.18E-02	leptin
Nucb2	-0.607	0.657	5.82E-03	nucleobindin 2
Rarres2	-0.610	0.655	1.97E-02	retinoic acid receptor responder (tazarotene induced) 2
Retnla	-0.779	0.583	5.44E-03	resistin like alpha
Sema3b	-0.605	0.658	1.88E-02	sema domain, immunoglobulin domain (Ig), short basic domain, secreted, (semaphorin) 3B
Sema3d	-0.677	0.625	2.55E-03	sema domain, immunoglobulin domain (Ig), short basic domain, secreted, (semaphorin) 3D
Sfrp2	-0.796	0.576	2.10E-03	secreted frizzled-related protein 2
Sfrp4	-1.293	0.408	3.35E-08	secreted frizzled-related protein 4
Smoc1	-0.542	0.687	1.18E-02	SPARC related modular calcium binding 1

Sparc	-0.490	0.712	2.03E-02	secreted acidic cysteine rich glycoprotein
Wnt2	-0.711	0.611	2.35E-02	wingless-type MMTV integration site family, member 2

Genes with unidentified function in the adipose tissue and non coding RNAs

AW551984	-0.645	0.640	4.93E-02	expressed sequence AW551984
Bcas1	-0.663	0.632	3.66E-02	breast carcinoma amplified sequence 1
C130074G19	-0.522	0.696	3.25E-02	RIKEN cDNA C130074G19 gene
Fam102b	-0.688	0.621	1.04E-03	family with sequence similarity 102, member B]
Fam114a1	-0.554	0.681	4.41E-02	family with sequence similarity 114, member A1
Fam171b	-0.759	0.591	1.58E-02	family with sequence similarity 171, member B
Gm10093	-0.809	0.571	2.36E-02	histone deacetylase 1 pseudogene
H19	-0.825	0.565	2.04E-04	H19, imprinted maternally expressed transcript (ncRNA)
Snhg18	-0.615	0.653	4.61E-02	small nucleolar RNA host gene 18 (ncRNA)
Zeb2os	-0.805	0.573	4.55E-03	inc finger E-box binding homeobox 2, opposite strand (ncRNA)

Genes with function described in other cell types

Gap43	-0.917	0.529	1.58E-03	growth associated protein 43
Kcnk2	-0.757	0.592	2.13E-02	potassium channel, subfamily K, member 2
Nbl1	-0.724	0.606	1.76E-02	neuroblastoma, suppression of tumorigenicity 1
Net1	-0.781	0.582	1.42E-03	neuroepithelial cell transforming gene 1
Nov	-0.859	0.551	1.77E-03	nephroblastoma overexpressed gene
Nrep	-0.517	0.699	3.95E-02	neuronal regeneration related protein
Ogn	-0.702	0.615	2.08E-03	osteoglycin
Plp1	-0.579	0.669	8.66E-03	proteolipid protein (myelin) 1
Sbsn	-0.727	0.604	3.65E-02	suprabasin
Sgms2	-0.650	0.637	2.34E-02	sphingomyelin synthase 2

GOTERM_BP_DIRECT	**Down regulated genes in the inguinal subcutaneous adipose tissue of 2-week-old *Egr1*$^{-/-}$ mice**	
	Enrichment scores / P-values	**Genes**
Collagen fibril organization	**23.8**/ 2.4^{E}-10	*Adamts2* a disintegrin-like and metallopeptidase (reprolysin type) with thrombospondin type 1 motif, 2 *Col1a1* collagen, type I, alpha 1 *Col1a2* collagen, type I, alpha 2 *Col3a1* collagen, type III, alpha 1 *Col5a2* collagen, type V, alpha 2 *Col14a1* collagen, type XIV, alpha 1 *Dpt* dermatopontin *Ddr2* discoidin domain receptor family, member 2 *Lum* lumican *Sfrp2* secreted frizzled-related protein 2
Collagen catabolic process	**21.1**/ 8^{E}-5	*Adamts2* a disintegrin-like and metallopeptidase (reprolysin type) with thrombospondin type 1 motif, 2 *Ctsk* cathepsin K *Mrc2* mannose receptor, C type 2 *Mmp14* matrix metallopeptidase 14 *Mmp2* matrix metallopeptidase 2
Extracellular matrix organization	**6.7**/ 6.1^{E}-4	*Adamtsl4* ADAMTS-like 4 *Smoc1* SPARC related modular calcium binding 1 *Ccdc80* coiled-coil domain containing 80 *Ecm2* extracellular matrix protein 2, female organ and adipocyte specific *Fn1* fibronectin 1 *Olfml2b* olfactomedin-like 2B *Postn* periostin
Ossification	**6.5**/ 2.2^{E}-3	*Bmp3* bone morphogenetic protein 3 *Chrdl1* chordin-like 1 *Ddr2* discoidin domain receptor family, member 2 *Igf2* insulin-like growth factor 2 *Lrrc17* leucine rich repeat containing 17

		Mmp14 matrix metallopeptidase 14
Wound healing	**5.6**/ 3.4^{E}-2	*Col1a1* collagen, type I, alpha 1 *Col3a1* collagen, type III, alpha 1 *Fgf2* fibroblast growth factor 2 *Fn1* fibronectin 1
Positive regulation of MAPK cascade	**4.5**/ 2.6^{E}-2	*Igf1* insulin-like growth factor 1 *Igf2* insulin-like growth factor 2 *Lep* leptin *Lpar1* lysophosphatidic acid receptor 1 *Timp2* tissue inhibitor of metalloproteinase 2
Cell adhesion	**3.2**/ 1.6^{E}-4	*Cd34* CD34 antigen *Alcam* activated leukocyte cell adhesion molecule *Cdh11* cadherin 11 *Col14a1* collagen, type XIV, alpha 1 *Dpt* dermatopontin *Emilin2* elastin microfibril interfacer 2 *Fap* fibroblast activation protein *Fn1* fibronectin 1 *Mfap4* microfibrillar-associated protein 4 *Nov* nephroblastoma overexpressed gene *Postn* periostin *Pcdh20* protocadherin 20 *Pcdhb14* protocadherin beta 14 *Srpx2* sushi-repeat-containing protein, X-linked 2 *Thbs3* thrombospondin 3 *Vcan* versican

Figure 3-figure supplement 2

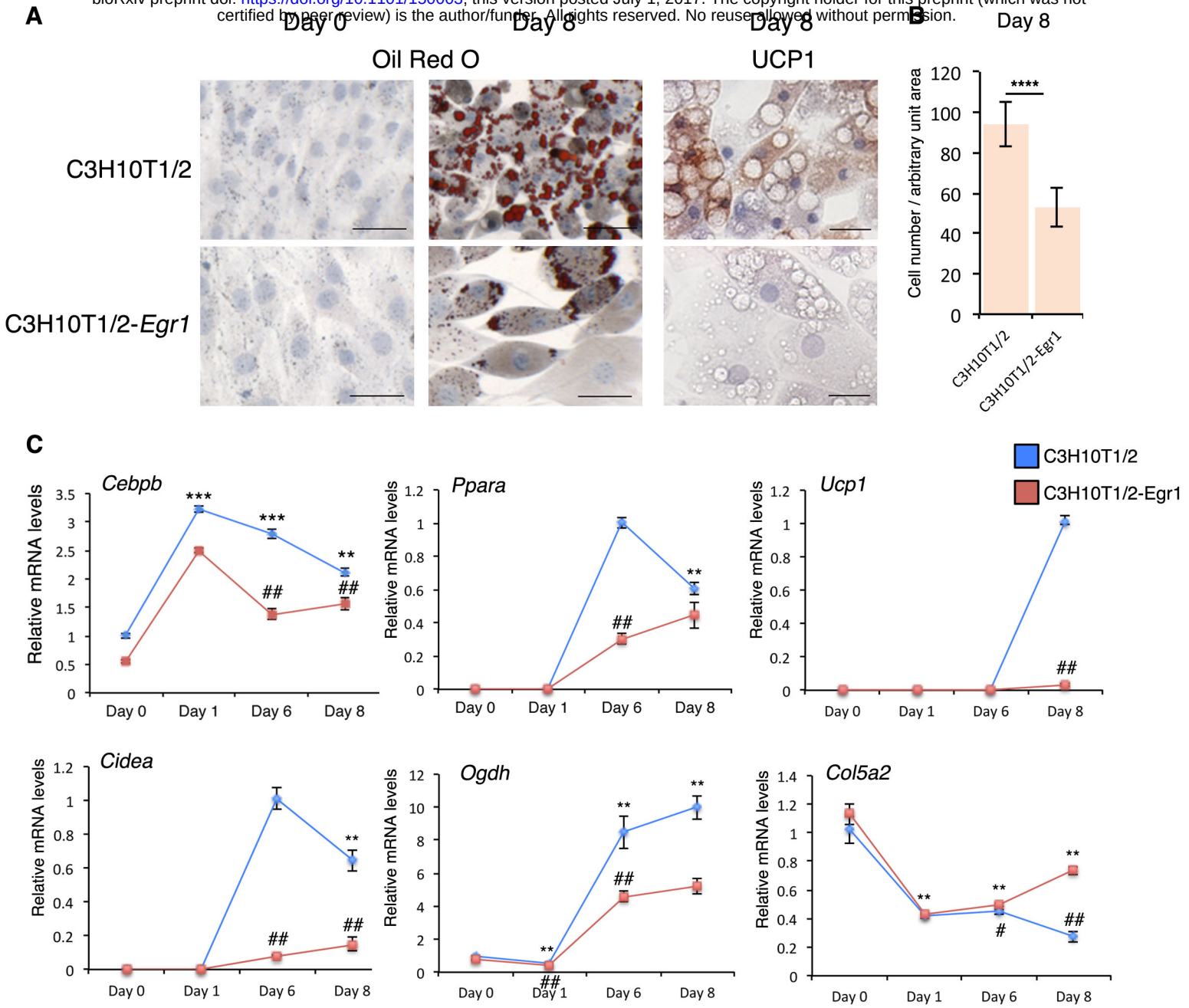

D EGR1 regulates SC-WAT browning through a direct recruitment to *Cebpb* and *Ucp1* promoters

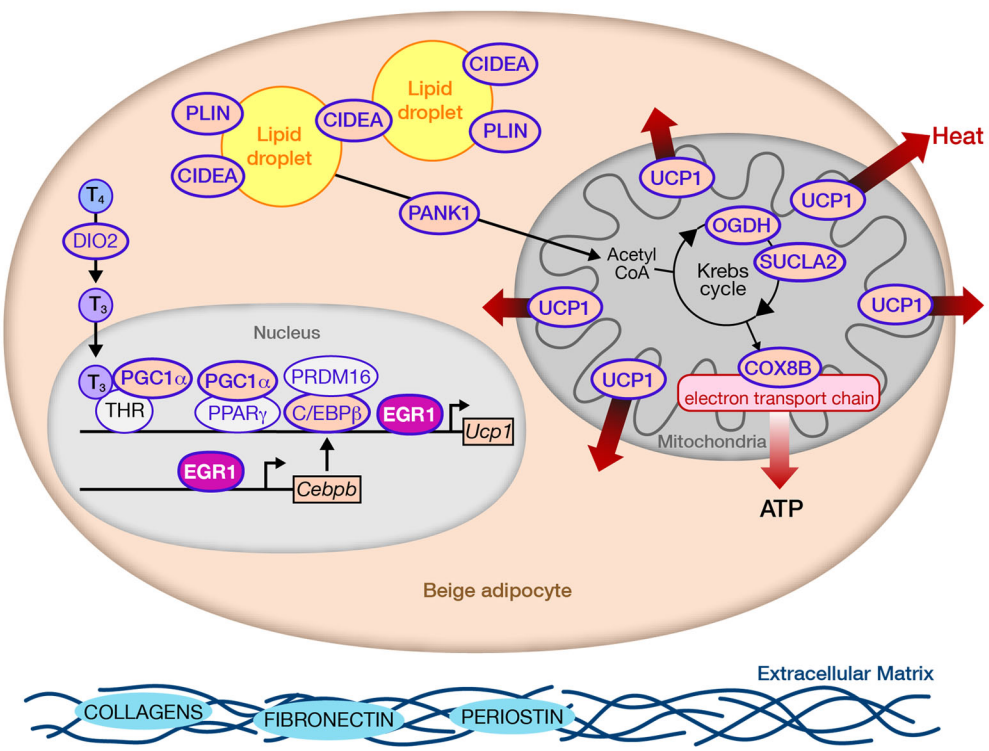

Figure 4

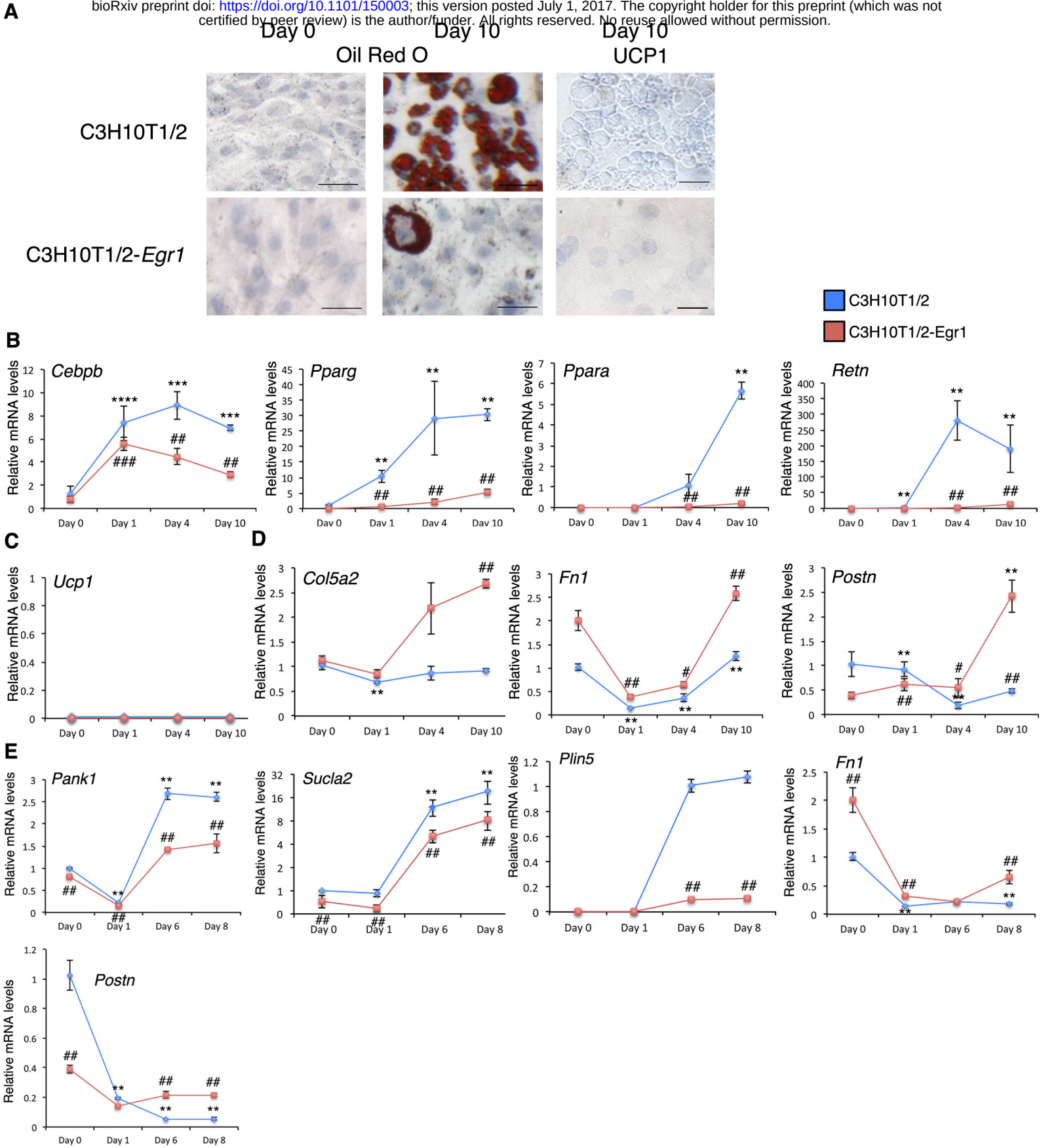

Figure 4-figure supplement 1

For RT-qPCR analysis		
Gene name	**Forward Primer**	**Reverse Primer**
Cebpb	5’- CGCCTTTAGACCCATGGAAG	5’- AGGCAGTCGGGCTCGTAGTAG
Ppara	5’-AACATCGAGTGTCGAATATGTGG	5’- CCGAATAGTTCGCCGAAAGAA
Pparg	5’- TCGGTGATGCACTGCCTATG	5’- GAGAGGTCCACAGAGCTGATT
Ppargc1a	5’- TGGACGGAAGCAATTTTTCA	5’- TTACCTGCGCAAGCTTCTCT
Dio2	5’- CTTCTCTACCACCACCTTC	5’- CATCTTCACCCAGTTTAACC
Pank1	5’- GTTCGCCCAGCATGATTCTC	5’- CTTAACCAGGGTTCCACCGAT
Cidea	5’- ACTTCCTCGGCTGTCTCAATGTCA	5’- TCAGCAGATTCCTTAACACGGCCT
Ucp1	5’- GGGCATTCAGAGGCAAATCAGCTT	5’- ACACTGCCACACCTCCAGTCATTA
Cox8b	5’- AGCCAAAACTCCCACTTCC	5’- TCTCAGGGATGTGCAACTTC
Plin5	5’- CAGAGCAAACACCGTACCCAG	5’- GGGATGGAAAGTAGGGCTAGG
Ogdh	5’- TATGGCCTACACGAGTCTGAC	5’- CCAGCCGACGGATGATCTCA
Sucla2	5’- ACCCTTTCGCTGCATGAATAC	5’- CTGTGCCTTTATCACAACATCCT
Col1a1	5’- TGGAGAGAGCATGACCGAT	5’- GAGCCCTCGCTTCCGTACT
Col5a2	5’- ACAGGTGAAGTGGGATTCTCA	5’- CCATAGCACCCATTGGACCA

Col14a1	5'- TGGAGTATTGGGAGGTTCAACT	5'- TGCCACTCTATTCTGGGGTCC
Fn1	5'- CACGTACCTCTTCAAAGTCTTTG	5'- GGATTGCTTTCCCTGCCCT
Postn	5'- TGGTATCAAGGTGCTATCTGCG	5'- AATGCCCAGCGTGCCATAAA
Dcn	5'- CTATGTGCCCCTACCGATGC	5'- CAGAACATGCACCACTCGAAG
Mmp2	5'- CAAGTTCCCCGGCGATGTC	5'- TTCTGGTCAAGGTCACCTGTC
Retn	5'- GCCATCGACAAGAAGATCAA	5'- CTTCCCTCTGGAGGAGACTG
βactin	5'- GATCTGGCACCACACCTTCT	5'- GGGGTGTTGAAGGTCTCAAA
Rplp0	5'- ACCTCCTTCTTCCAGGCTTT	5'- CTCCCACCTTGTCTCCAGTC
18S	5'- GGCGACGACCCATTCG	5'- ACCCGTGGTCACCATGGTA
For ChIP-qPCR analysis		
Promoter name	**Forward Primer**	**Reverse Primer**
Cebpb	5'- GAGGGAACTCAGAAGCAAAGT	5'- AGCCCTCCACCCTATGTAT
Ppargc1a	5'- GCCTATGAGATCCACGGAAAG	5'- GTCTCCTTGGCAGTAGAGAATG
Ucp1	5'- TGTGGCCAGGGCTTTGGGAGT	5'- AGATTGCCCGGCACTTCTGCG
Gapdh	5'- CAGGAGCCCAGGGAAGATACAAATA	5'- ACGCATACACATATACAACCAGTCA

Supplementary Table 1